Electronic Supplementary Material (ESI) for Inorganic Chemistry Frontiers.

Electronic Supplementary Information

Strain-Based Design, Direct Macrocyclization, and Metal Complexation of Thiazole-Containing Calix[3]pyrrole Analogues

Keita Watanabe,[a] Kotaro Shibata,[a] Tomoya Ichino,*[b] Yuki Ide,[b] Tomoki Yoneda,[a] Satoshi Maeda,[b,c] and Yasuhide Inokuma*[a,b]

[a] Division of Applied Chemistry, Faculty of Engineering, Hokkaido University, Kita 13, Nishi 8, Kita-ku, Sapporo, Hokkaido, 060-8628, Japan.

[b] Institute for Chemical Reaction Design and Discovery (WPI-ICReDD), Hokkaido University, Kita-21, Nishi 10, Kita-ku, Sapporo, Hokkaido, 001-0021, Japan

[c] Department of Chemistry, Faculty of Science, Hokkaido University, Kita 10, Nishi 8, Kita-ku, Sapporo, Hokkaido, 060-8610, Japan.

Correspondence to: tichino@eis.hokudai.ac.jp; inokuma@eng.hokudai.ac.jp

Table of Contents

1. General Information

Solvents and reagents were purchased from WAKO Pure Chemical Industries Ltd., TCI Co., Ltd., Kanto Chemical Co., Inc., or Sigma-Aldrich Co., and used without further purification unless otherwise mentioned. Compound **6** was prepared according to a reported procedure.[1] All ^{1}H and ^{13}C NMR spectra were recorded using JEOL JMN-ECS400 spectrometer and chemical shifts were reported in parts per million (ppm) relative to an internal standard tetramethylsilane (δ = 0.00 ppm for ^{1}H NMR in $CDCl_3$) or a solvent residual peak (δ = 77.16 ppm for ^{13}C NMR in $CDCl_3$, δ = 1.94 ppm for ^{1}H NMR in CD_3CN, δ = 1.32 ppm for ^{13}C NMR in CD_3CN). Infrared spectra were measured using a JASCO Co. FT/IR-4600. ESI-TOF-MS spectra were recorded on a Thermo Scientific Executive spectrometer. Thin layer chromatography was performed on silica gel sheets, MERCK silica gel 60 F254. Preparative scale separations were performed by means of gravity column chromatography over silica gel (Wakosil® 60. 64 ~ 210 μm). Single crystal X-ray diffraction data were obtained using Rigaku XtaLAB P200 diffractometer equipped with a PILATUS200K detector, which uses a multilayer mirror (MoK_α radiation λ = 0.71073 Å or CuK_α radiation λ = 1.54184 Å). UV–vis absorption spectra were recorded on a Shimadzu UV-1800 spectrophotometer. Analytical HPLC chromatograms were recorded using a JASCO MD-2018 photodiode array detector quipped with a JASCO PU-2089 pump, JASCO AS-2059 sampler, and JASCO CO-2060 column thermostat. All structures were solved using a dual-space algorithm (SHELXT) and refined using full-matrix least-squares methods (SHELXL).[2,3]

2. Synthetic Procedures

2.1 Synthesis of Compound 5

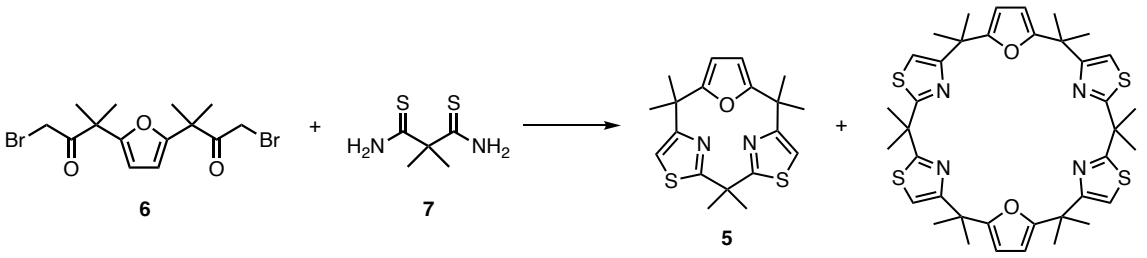

In a 1 L round-bottomed flask equipped with a reflux condenser, compounds **6** (588 mg, 1.5 mmol) and **7** (244 mg, 1.5 mmol) were dissolved in ethanol (600 mL). The resulting solution was then refluxed for 19 h. After cooling the solution, the solvent was evaporated using a rotary evaporator. The residue was dissolved in dichloromethane (40 mL), and the solution was neutralized with saturated aqueous solution of sodium bicarbonate (30 mL). The biphasic solution was transferred to a separation funnel, and the organic layer was separated. The remaining aqueous layer was extracted with dichloromethane (30 mL × 3), and the combined organic layer was washed with a saturated aqueous solution of sodium bicarbonate (30 mL × 2), and then with water (30 mL). After drying the organic layer over anhydrous sodium sulfate, the solvent was removed by evaporation to leave an oily solid. The residue was chromatographed on silica gel (column diameter: 4.2 cm, height: 17 cm, eluent: hexane/ethyl acetate = 30/1) and the fraction at R_f = 0.20 was collected to give compound **5** (320 mg, 60% yield) as a colorless solid.

Characterization data for **5**

^{1}H NMR ($CDCl_3$, 400 MHz, 298 K): δ 6.78 (s, 2H, thiazolyl), 5.88 (s, 2H, furyl), 1.93 (s, 6H, dimethylmethylene), 1.63 ppm (s, 12H, dimethylmethylene); ^{13}C NMR ($CDCl_3$, 100 MHz, 298 K): δ 175.8, 163.2, 161.2, 110.2, 103.2, 47.9, 40.6, 27.6, 26.0 ppm; IR (ATR, neat): 3101, 2964, 2924, 2863, 1505, 1456, 1442, 1378, 1362, 1297, 1260, 1244, 1200, 1159, 1118, 1097, 1073, 1048, 1022, 1009, 953 cm^{-1}; HR-ESI-TOF-MS (*m/z*): $[M+H]^+$ calcd. for $C_{19}H_{23}N_2OS_2$, 359.1246, found, 359.1239; TLC (hexane : ethyl acetate, 30:1 v/v): R_f = 0.20.

Isolation and Characterization of **14**

Compound **14** (R_f = 0.30) was isolated in 16% yield (146 mg) on a scale starting from 980 mg of compound **6** by silica gel column chromatography.

^{1}H NMR ($CDCl_3$, 400 MHz, 298 K): δ 6.43 (s, 4H, thiazolyl), 5.99 (s, 4H, furyl), 1.84 (s, 12H, dimethylmethylene), 1.65 ppm (s, 24H, dimethylmethylene); ^{13}C NMR ($CDCl_3$, 100 MHz, 298 K): δ 175.5, 162.3, 159.7, 112.7, 104.3, 46.4, 39.8, 29.9, 27.3 ppm; IR (ATR, neat): 2965, 2359, 1550, 1500, 1458, 1377, 1359, 1258, 1199, 1075, 1013 cm^{-1}; HR-ESI-TOF-MS (*m/z*): $[M+H]^+$ calcd. for $C_{38}H_{45}N_4O_2S_4$. 717.2420, found, 717.2403; TLC (hexane : ethyl acetate, 30:1 v/v): R_f = 0.30.

2.2 Synthesis of 8 and 2

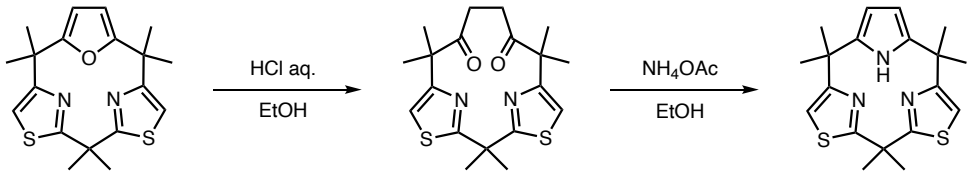

5 8 2

Compound **5** (336 mg, 0.94 mmol) was dissolved in a mixture of 12 M HCl (40 mL) and ethanol (30 mL) in a 200 mL round-bottomed flask. After connecting a reflux condenser to the flask, the solution was heated at 100 ºC for 2 d. The reaction mixture was then cooled to room temperature, and the reaction solution was poured into aqueous solution of sodium bicarbonate (200 mL). Diethyl ether (200 mL) was added to the mixture to form a two-phase system. After the organic layer was separated, the aqueous layer was extracted twice with diethyl ether (200 mL). The combined organic layer was washed successively with saturated aqueous solution of sodium bicarbonate (200 mL) and water (200 mL), then dried over anhydrous sodium sulfate. Evaporation of the solvent under reduced pressure gave almost pure **8** that was used for the next reaction without further purification.

The resulting compound **8** was transferred into a 100 mL round-bottomed flask equipped with a reflux condenser, and ammonium acetate (3.08 g, 40 mmol) was added. The solid mixture was suspended in ethanol (30 mL), and then heated to reflux for 1 d during which all solids were dissolved to give a homogeneous solution. After cooling the solution, the solvent was evaporated. The residue was dissolved in diethyl ether (50 mL) and water (50 mL). The organic layer was separated, and the aqueous layer was extracted with diethyl ether (30 mL × 3). The combined organic layer was washed with water (30 mL × 2), brine (30 mL), and dried over anhydrous sodium sulfate. After evaporation of the solvent, the mixture was purified using silica gel column chromatography (column diameter: 3.0 cm, height: 12 cm, eluent: hexane/ethyl acetate = 20/1) to give calix[1]pyrrole[2]thiazole **2** (262 mg, 78% yield from **5**) as a colorless solid.

Characterization data for **8**

For characterization of **8**, crude **8** was purified by reprecipitation from hexane to give an analytical sample.

^{1}H NMR ($CDCl_3$, 400 MHz, 298 K): δ 6.93 (s, 2H, thiazolyl), 2.32 (s, 4H, ethylene), 1.90 (s, 6H, dimethylmethylene), 1.41 ppm (s, 12H, dimethylmethylene); ^{13}C NMR ($CDCl_3$, 100 MHz, 298 K): δ 212.9, 177.4, 161.0, 111.6, 51.7, 46.2, 33.3, 29.3, 23.8 ppm; IR (ATR, neat): 3117, 2967, 2927, 1704, 1507, 1462, 1435, 1381, 1361, 1309, 1261, 1248, 1211, 1161, 1084, 1058, 1030, 1011, 995 cm^{-1}; HR-ESI-TOF-MS (*m/z*): $[M+Na]^+$ calcd. for $C_{19}H_{24}N_2O_2S_2Na$, 399.1171, found, 399.1163; TLC (hexane : ethyl acetate, 5:1 v/v): R_f = 0.47.

Characterization data for **2**

^{1}H NMR ($CDCl_3$, 400 MHz, 298 K): δ 12.17 (brs, 1H, NH), 6.57 (s, 2H, thiazolyl), 5.53 (d, ^{4}J = 2.3 Hz, 2H, pyrrolyl), 2.13 (s, 6H, dimethylmethylene), 1.77 ppm (s, 12H, dimethylmethylene); ^{13}C NMR($CDCl_3$, 100 MHz, 298 K): δ 174.8, 165.4, 140.3, 109.9, 99.99, 46.9, 39.2, 26.8, 26.2 ppm; IR (ATR, neat): 3255, 2961, 2921, 1557, 1506, 1456, 1381, 1357, 1294, 1215, 1065, 1050 cm^{-1}; HR-ESI-TOF-MS (*m/z*): $[M+H]^+$ calcd. for $C_{19}H_{24}N_3S_2$, 358.1406, found, 358.1400; TLC (hexane : ethyl acetate, 20:1 v/v): R_f = 0.32.

2.3 Synthesis of 10 and 15

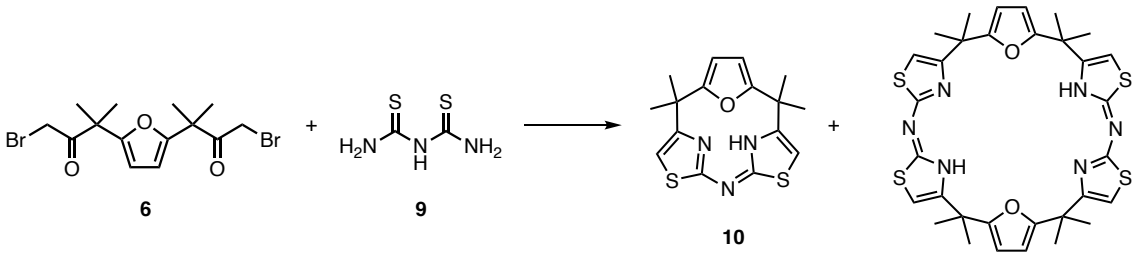

According to the synthetic procedure described for compounds **5** and **14**, reaction between precursor **6** (499 mg, 1.26 mmol) and **9** (170 mg, 1.26 mmol) was carried out to give a crude reaction mixture containing **10** and **15**.

Isolation of Compound **10** and **15**

Upon addition of a mixture of dichloromethane and methanol (v/v=40/1, *ca*. 3 mL) to the reaction mixture, compound **15** precipitated as a colorless powder. The precipitate was collected by filtration to give **15** (133 mg, 32%). The filtrate containing **10** was chromatographed on silica gel (column diameter: 3.0 cm, height: 15 cm, eluent: dichloromethane/methanol = 40/1) to collect fractions at R_f = 0.4~0.5. The resulting mixture was further purified by silica gel column chromatography (column diameter: 1.5 cm, height: 25 cm, eluent: dichloromethane/ethyl acetate = 20/1) to obtain compound **10** (7.5 mg, 2%) as a pale yellow solid with an R_f of 0.4.

Characterization data for **10**

^{1}H NMR ($CDCl_3$, 400 MHz, 298 K): δ 18.7 (brs, 1H, NH), 6.13 (s, 2H, thiazolyl), 5.97 (s, 2H, furyl), 1.74 (s, 12H, dimethylmethylene) ppm; ^{13}C NMR ($CDCl_3$, 100 MHz, 298 K): δ 171.2, 160.8, 149.7, 106.6,100.0, 40.4, 24.9 ppm; IR (ATR, neat): 3112, 2963, 1443, 1365, 1258, 1084, 1013, 953, 862, 791 cm^{-1}; HR-ESI-TOF-MS (*m/z*): $[M+H]^+$ calcd. for, $C_{16}H_{18}N_3OS_2$, 332.0886, found, 332.0880; TLC (dicloromethane : ethyl acetate, 20:1 v/v): R_f =0.50.

Characterization data for **15**

In $CDCl_3$, compound **15** exhibited two sets of signals attributable to tautomers for the *N*-bridged bis(thiazole) units.

^{1}H NMR ($CDCl_3$, 400 MHz, 298 K): major tautomer: δ 6.16 (brs, 4H, thiazolyl), 6.00 (s, 4H, furyl), 1.60 (s, 24H, dimethylmethylene) NH protons were not observed due to signal broadening; minor tautomer: 12.76 (brs, NH, 2H), 6.22 (s, 4H, thiazolyl), 5.80 (s, 4H, furyl), 1.55 (s, 24H, dimethylmethylene) ppm; IR (ATR, neat): 3110, 2969, 1558, 1511, 1430, 1376, 1299, 1254, 1200, 1152, 1118, 1096, 1034, 955 cm^{-1}; HR-ESI-TOF-MS (*m/z*): $[M+H]^+$ calcd. for $C_{45}H_{29}ONS_2$, 663.1685, found, 663.1688; TLC (dichloromethane : methanol, 40:1 v/v): R_f = 0.40.

2.4 Synthesis of Zn complex 11

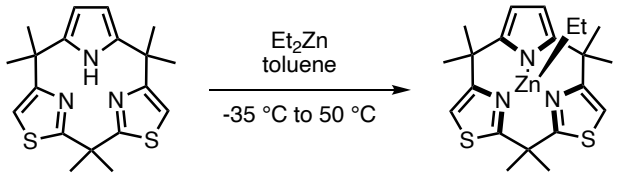

2 **11**

In a 10 mL Schlenk tube, ligand **2** (35.7 mg, 100 μmol) was dissolved in dry toluene (0.6 mL) under N_2 atmosphere. After the solution was cooled to –35 °C, 200 μL of 1.0 M toluene solution of $ZnEt_2$ (200 μmol) was added via syringe. Then the solution was stirred at 50 °C for 16 h. After cooling the solution to room temperature, 7 mL of toluene was added to the mixture. White precipitate was removed by filtration, and the filtrate was evaporated to leave crude **11** as an yellow solid. The solid was washed with 3 mL of hexane on a funnel to give complex **11** (32.4 mg) in 72% yield as a greenish yellow powder.

^{1}H NMR($CDCl_3$, 400 MHz, 298 K): δ 6.68 (s, 2H, thiazolyl), 5.66 (s, 2H, pyrrolyl), 2.24 (s, 3H, dimethylmethylene), 1.98 (overlapped, 9H, dimethylmethylene), 1.76 (s, 6H, dimethylmethylene), 1.37 (t, ^3J = 8.1 Hz, 3H, $ZnCH_2CH_3$), 0.54 ppm (q, ^3J = 8.1 Hz, 2H, $ZnCH_2CH_3$); ^{13}C NMR ($CDCl_3$, 100 MHz, 298 K): δ 174.1, 166.8, 143.8, 109.9, 101.0, 46.2, 40.7, 27.8, 26.6, 25.6, 24.4, 13.1, 1.1 ppm; IR (ATR, neat): 3087, 2968, 2923, 2874, 2832, 1508, 1358, 1211, 1078, 1055 cm^{-1}; HR-ESI-TOF-MS (*m/z*): $[M+H]^+$ calcd. for $C_{21}H_{27}N_3S_2Zn$, 450.1011, found, 450.1008.

2.5 Synthesis of Pd complex 12

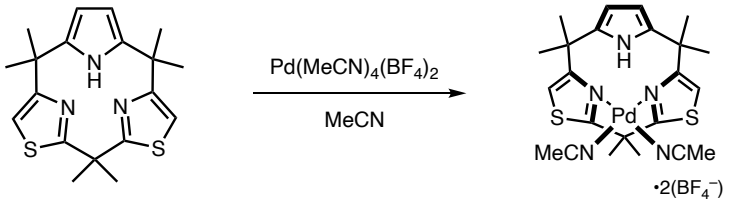

2 **12**

In a 50 mL round-bottomed flask, ligand **2** (71.4 mg, 200 μmol) and tetrakis(acetonitrile)palladium(II) tetrafluoroborate (88.8 mg, 200 μmol) were dissolved in acetonitrile (7 mL), and the solution was stirred for 30 min at room temperature. Then diethyl ether (35 mL) was added to the solution, leading to the formation of brown precipitate. The precipitate was collected by filtration, washed with diethyl ether (10 mL), and dried in a desiccator under reduced pressure overnight to give complex **12** (62.2 mg, 43% yield) as brown powder.

^{1}H NMR(CD_3CN, 400 MHz, 298 K): δ 8.31 (brs, 1H, NH), 7.68 (s, 2H, thiazolyl), 6.72 (d, ^{4}J = 2.8 Hz, 2H, pyrrolyl), 3.24 (s, 3H, dimethylmethylene), 2.37 (s, 6H, PdNCCH_3), 2.27 (s, 3H, dimethylmethylene), 1.74 (s, 6H, dimethylmethylene), 1.69 ppm (s, 6H, dimethylmethylene); ^{13}C NMR (CD_3CN, 100 MHz, 298 K): δ 175.4, 163.5, 139.1, 120.6, 118.6, 110.3, 52.6, 41.4, 32.3, 32.1, 28.1, 27.6, 4.2 ppm; IR (ATR, neat): 3350, 3124, 2980, 1626, 1514, 1469, 1392, 1366, 1241, 1194, 1016, 876, 788, 763 cm^{-1}; HR-ESI-TOF-MS (*m/z*): $[M\text{-}2BF_4^-]^{2+}$ calcd. for $C_{23}H_{29}N_5{}^{102}PdS_2$, 270.5455, found, 270.5454.

3. X-ray Crystallographic Analysis

3.1 Crystallographic data for calix[1]furan[2]thiazole•TFA (5•TFA)

Single crystal suitable for X-ray diffraction analysis were grown by vapor diffusion of hexane into a dichloromethane and TFA solution of **5**.

$C_{23}H_{24}F_6N_2O_5S_2$, M = 586.56, crystal size: 0.31 × 0.17 × 0.10 mm^3, triclinic, space group P_1, a = 10.5263(4), b = 11.7269(7), c = 12.6306(8) Å, α = 114.566(6), β = 109.613(5), γ = 93.736(4)°, V = 1297.04(14) Å^3, Z = 2, T = 123(2) K, μ = 0.286 mm^{-1}, D_{calc} = 1.502 g/cm^3, 1.934° ≤ θ ≤ 26.500°, 4541 unique reflections out of 5367 with $I > 2\sigma(I)$, GOF = 1.050, R_1 = 0.0436, wR_2 = 0.1263, CCDC: 2326011.

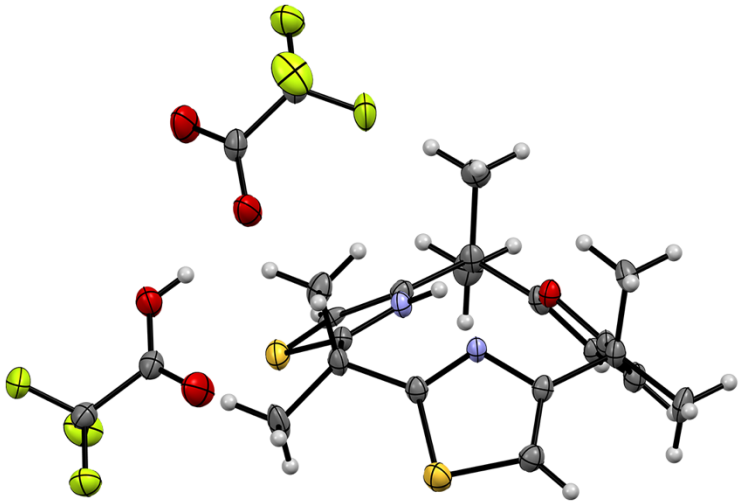

Figure S1. Crystal structure of compound **5•TFA**.

3.2 Crystallographic data for compound 8

Single crystal suitable for X-ray diffraction analysis were grown by vapor diffusion of hexane into a dichloromethane solution of **8**.

$C_{19}H_{24}N_2O_2S_2$, M = 376.52, crystal size: 0.14 × 0.06 × 0.03 mm^3, monoclinic, space group $P2_1/c$, a = 9.3949(4), b = 17.3945(7), c = 11.4391(5) Å, β = 101.562(4)°, V = 1831.44(14) Å^3, Z = 4, T = 123(2) K, μ = 0.306 mm^{-1}, D_{calc} = 1.366 g/cm^3, 2.162° ≤ θ ≤ 26.000°, 3239 unique reflections out of 3608 with $I > 2\sigma(I)$, GOF = 1.047, R_1 = 0.0325, wR_2 = 0.0839, CCDC: 2326012.

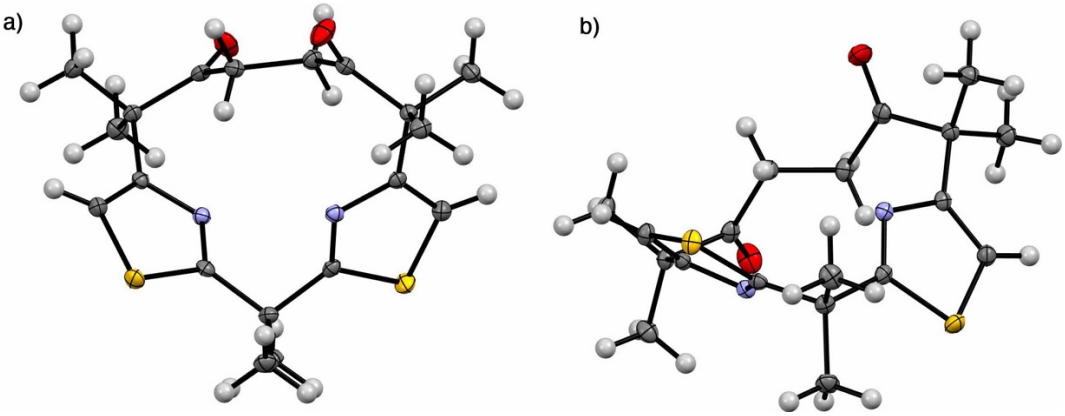

Figure S2. Crystal structure of compound **8**. a) Top view and b) side view.

3.3 Crystallographic data for calix[1]pyrrole[2]thiazole (2)

Single crystal suitable for X-ray diffraction analysis were grown from a H_2O/MeOH solution of **2** by slow evaporation.

$C_{19}H_{23}N_3S_2$, M = 357.52, crystal size: 0.66 × 0.31 × 0.30 mm^3, orthorhombic, space group *Pnma*, a = 10.3920(3), b = 17.1911(6), c = 10.2184(4) Å, V = 1825.52(11) Å^3, Z = 8, T = 123 K, μ = 0.297 mm^{-1}, D_{calc} = 1.301 g/cm^3, 2.319° ≤ θ ≤ 30.855°, 2259 unique reflections out of 2538 with $I > 2\sigma(I)$, GOF = 1.129, R_1 = 0.0830, wR_2 = 0.2616, CCDC: 2326013.

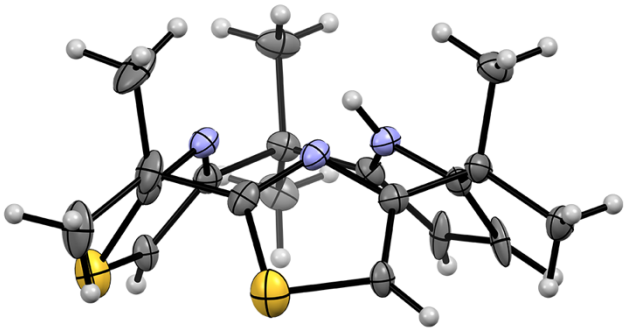

Figure S3. Crystal structure of compound **2**.

3.4 Crystallographic data for *meso*-N calix[1]furan[2]thiazole (10)

Single crystal suitable for X-ray diffraction analysis were grown by vapor diffusion of hexane into a dichloromethane solution of **10**.

$C_{16}H_{17}N_3OS_2$, M = 331.44, crystal size: 0.37 × 0.03 × 0.02 mm^3, monoclinic, space group $P2_1/n$, a = 10.1719(9), b = 13.9928(7), c = 11.8029(9) Å, β = 112.856(10)°, V = 1548.0(2) Å^3, Z = 4, T = 123(2) K, μ = 0.349 mm^{-1}, D_{calc} = 1.422 g/cm^3, 2.251° ≤ θ ≤ 27.496°, 3057 unique reflections out of 3507 with $I > 2\sigma(I)$, GOF =1.057, R_1 = 0.0464, wR_2 = 0.1044, CCDC: 2326014.

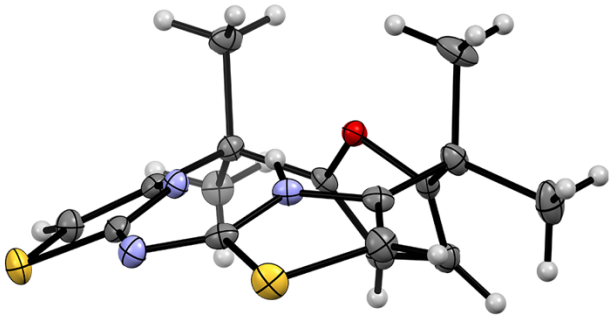

Figure S4. Crystal structure of compound **10**.

3.5 Crystallographic data for Zn complex (11)

Single crystal suitable for X-ray diffraction analysis were grown from a hexane solution of **11** by slow evaporation.

$C_{21}H_{27}N_3S_2Zn$, M = 450.94, crystal size: 0.12 × 0.06 × 0.04 mm^3, orthorhombic, space group $Pna2_1$, a = 13.2699(6), b = 10.7612(6), c = 14.5080(8) Å, V = 2071.74(19) Å^3, Z = 4, T = 123(2) K, μ = 1.398 mm^{-1}, D_{calc} = 1.446 g/cm^3, 2.356° ≤ θ ≤ 30.695°, 3900 unique reflections out of 4232 with $I > 2\sigma(I)$, GOF = 1.091, R_1 = 0.0376, wR_2 = 0.1015, CCDC: 2326015.

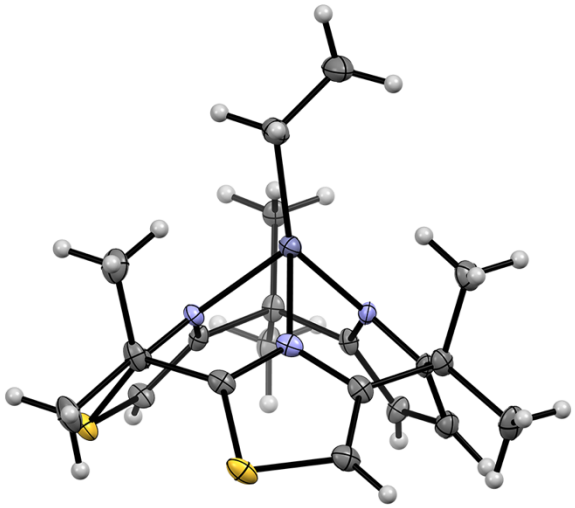

Figure S5. Crystal structure of Zn complex **11**.

3.6 Crystallographic data for Pd complex (12)

Single crystal suitable for X-ray diffraction analysis were grown by vapor diffusion of diethyl ether into an acetonitrile solution of **12**.

$C_{23}H_{29}B_2F_8N_5PdS_2$, M = 719.65, crystal size: 0.50 × 0.18 × 0.09 mm^3, monoclinic, space group $C2/c$, a = 20.2077(8), b = 14.5806(6), c = 21.4792(10) Å, β = 113.960(5)°, V = 5783.3(5) Å^3, Z = 8, T = 123(2) K, μ = 0.862 mm^{-1}, D_{calc} = 1.653 g/cm^3, 1.780° ≤ θ ≤ 30.817°, 6425 unique reflections out of 7153 with $I > 2\sigma(I)$, GOF = 1.070, R_1 = 0.0363, wR_2 = 0.0938, CCDC: 2326016.

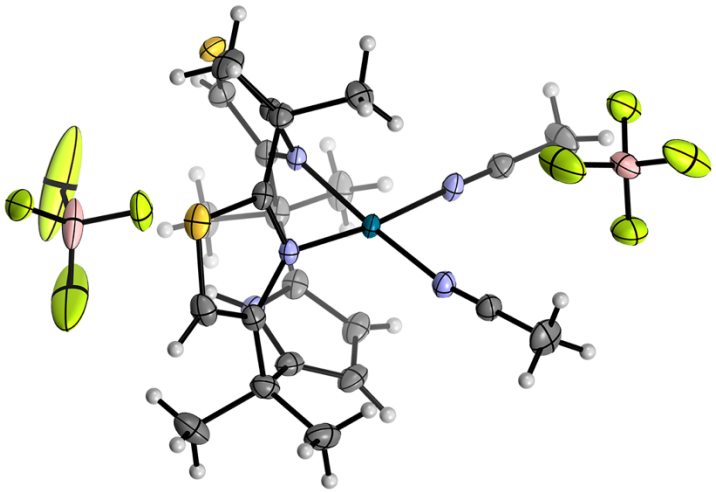

Figure S6. Crystal structure of Pd complex **12**.

3.7 Crystallographic data for Ag complex (13)

Single crystal suitable for X-ray diffraction analysis were grown by vapor diffusion of diethyl ether into an acetonitrile solution of **13**.

$C_{40}H_{49}AgBF_4N_7S_4$, M = 950.78, crystal size: 0.40 × 0.14 × 0.03 mm^3, orthorhombic, space group *Aba*2, a = 18.1946(9), b = 17.4102(8), c = 27.3255(11) Å, V = 8655.9(7) Å^3, Z = 8, T = 123(2) K, μ = 0.714 mm^{-1}, D_{calc} = 1.459 g/cm^3, 1.7822° ≤ θ ≤ 30.9555°, 8254 unique reflections out of 9034 with $I > 2\sigma(I)$, GOF = 1.013, R_1 = 0.0295, wR_2 = 0.0762, CCDC: 2326017.

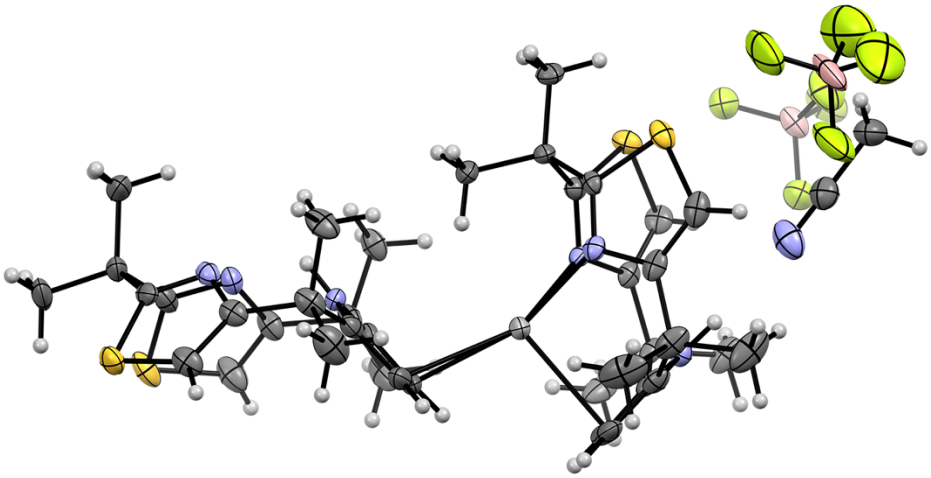

Figure S7. Crystal structure of Ag complex **13**.

4. Computational studies

4.1 Computational details

Conformational sampling: Systematic conformational search calculations of the calix[3]pyrrole (**1**) and the analogues (**2**–**5**, and **10**) were performed by the artificial force induced reaction method implemented in the global reaction route mapping (GRRM) grogram.[4,5] The model collision energy parameter (γ) was consistently set to 100.0 kJ/mol in the conformational search calculations. The total energies were estimated by the semi-empirical PM6 method[6] during these search calculations. The structures of all obtained conformers were optimized by the density functional theory (DFT) method at the M06-2X[7]/6-311+G(2d,p) level of theory to determine the lowest energy conformational structure. The relative stability was estimated by Gibbs free energy under standard condition. All energy calculations were carried out by the Gaussian 16 program.[8]

Visualization of ring strain: For the lowest energy DFT structures of the conformers **1**–**5**, and **10**, the evaluations of ring strain were performed by combinations of the StrainViz[9] and Gaussian 16 programs at the same DFT level of theory as the geometry optimization calculations. The distribution of strain energy was visualized by the visual molecular dynamics (VMD) software.[10] The initial and optimized structures of fragments were supplementarily summarized in Figures S15-S20.

*Visualization of non-covalent interaction in Pd complex **12***: The arrangements of heavy atoms were fixed at those in the crystal structure. The hydrogen atoms were fully optimized at the M06-2X/SDD (Pd)[11] and 6-31+G(d) (the others) level of theory by the GRRM program combined with the Gaussian 16 program. The single point calculation was carried out at the M06-2X/SDD (Pd) and 6-311+G(2d,p) (the others) level of theory to generate the wavefunction file required for the visualization of non-covalent interactions by the NCIPLOT program.[12] The non-covalent interaction was visualized by the VMD software. The M06-2X functional was selected in this analysis since this DFT functional performed the good description of anion$\cdots\pi$ interactions.[13]

Evaluation of conformational stability and ring strain at different computational levels: For **3** and **5**, the relative stability of low-lying energy conformers was investigated using three additional DFT functionals (B3LYP+D3,[14] *w*B97-XD,[15] and M06[7]). The comparative results are summarized in Table S1.

In order to confirm the computational identification of less-strained macrocycle, the StrainViz analysis was performed at the B3LYP+D3[14]/6-311+G(2d,p) level of theory. The optimized structures of the partial conformer for **1** and cone conformers for **2** and **4** were selected. The results are shown in Figure S23.

4.2 Optimized structures and relative stability of conformers

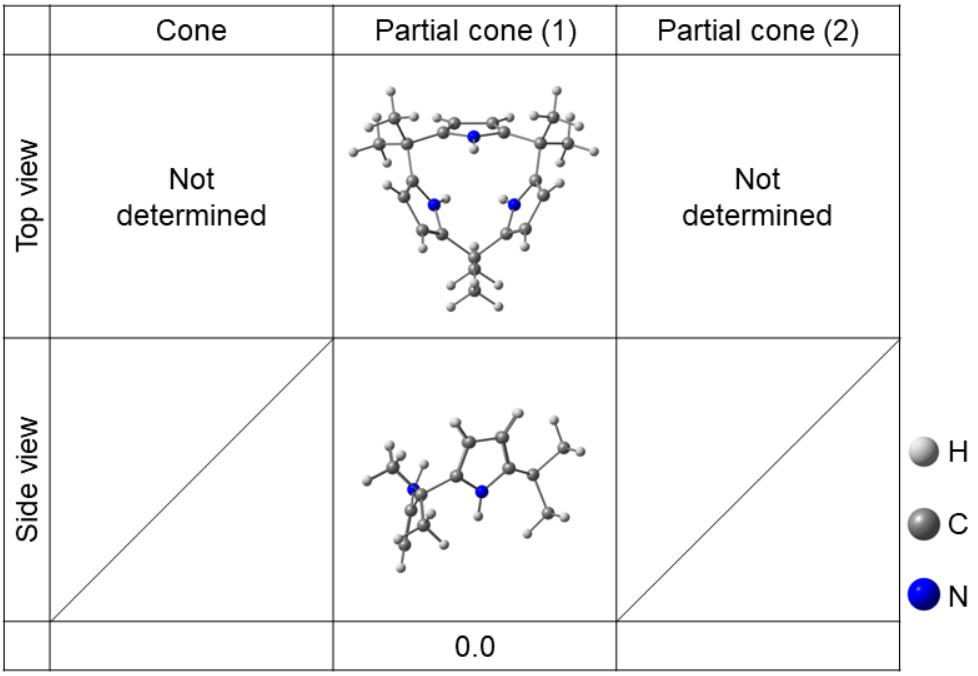

Figure S8. Optimized structures and relative free energies (kcal/mol) for conformers of compound **1**. Selected hydrogen bonding distances (Å) are also shown.

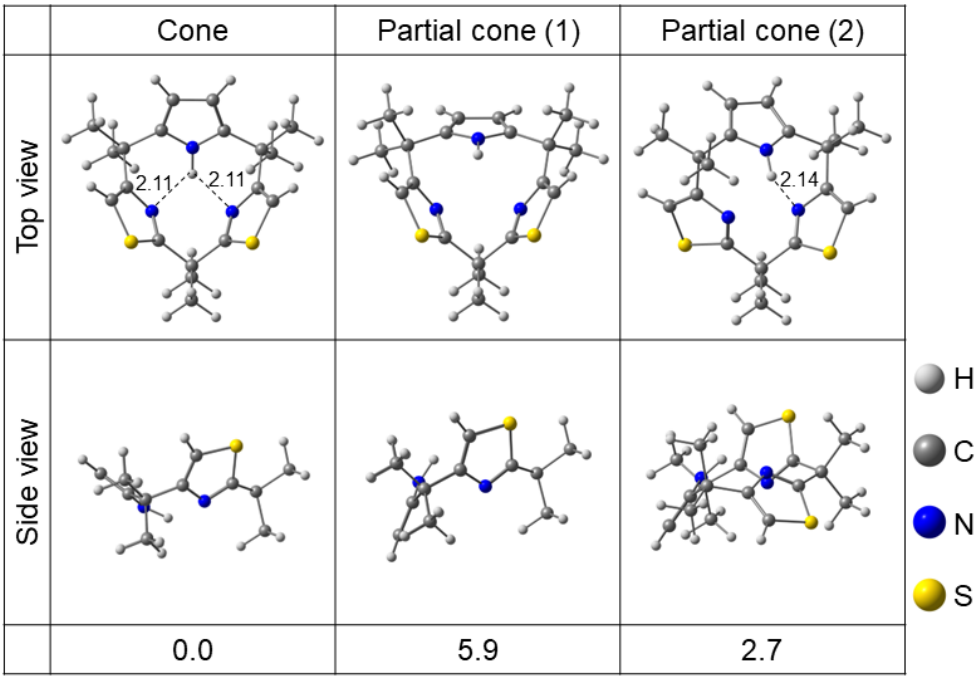

Figure S9. Optimized structures and relative free energies (kcal/mol) for conformers of compound **2**. Selected hydrogen bonding distances (Å) are also shown.

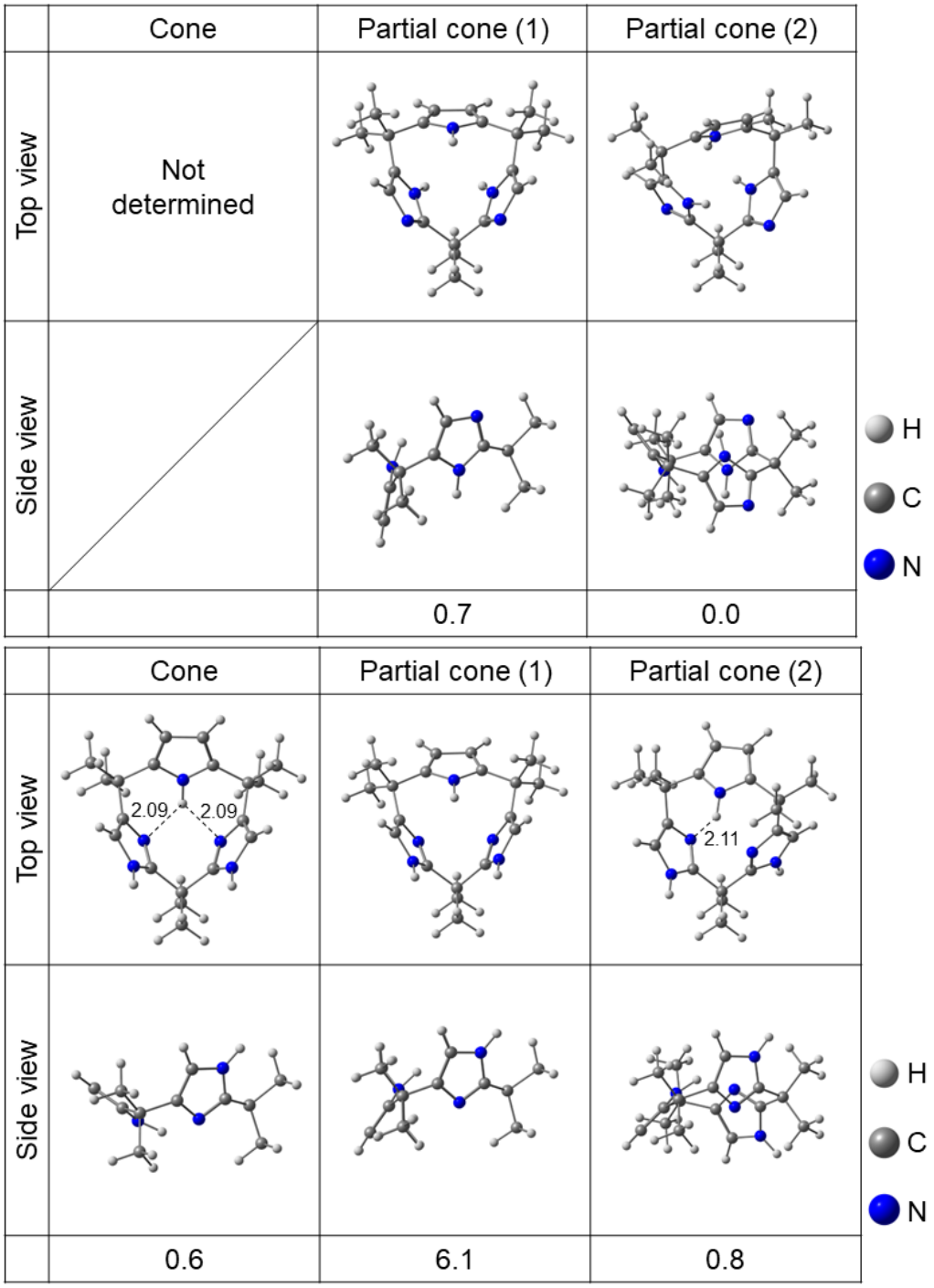

Figure S10. Optimized structures and relative free energies (kcal/mol) for conformers of compound **3**. Selected hydrogen bonding distances (Å) are also shown.

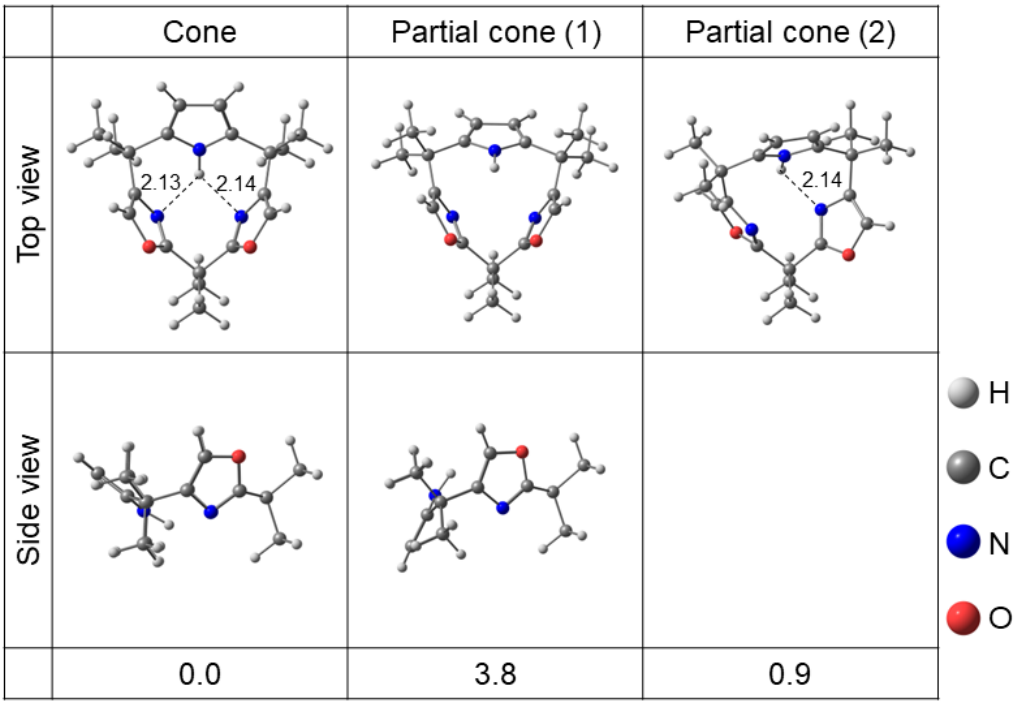

Figure S11. Optimized structures and relative free energies (kcal/mol) for conformers of compound **4**. Selected hydrogen bonding distances (Å) are also shown.

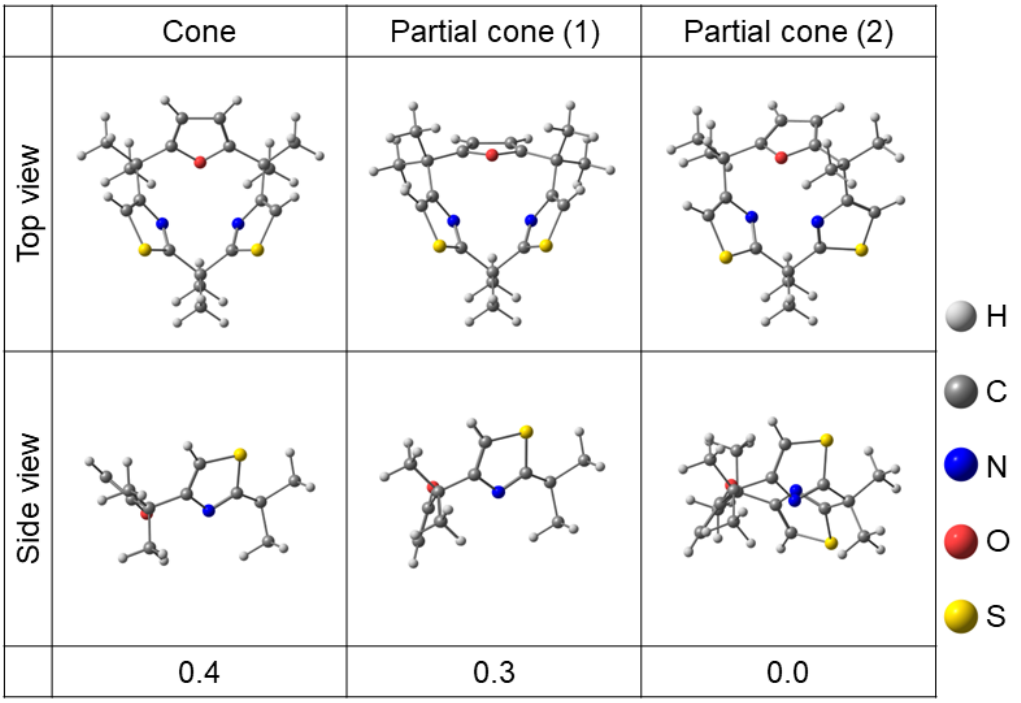

Figure S12. Optimized structures and relative free energies (kcal/mol) for conformers of compound **5**. Selected hydrogen bonding distances (Å) are also shown.

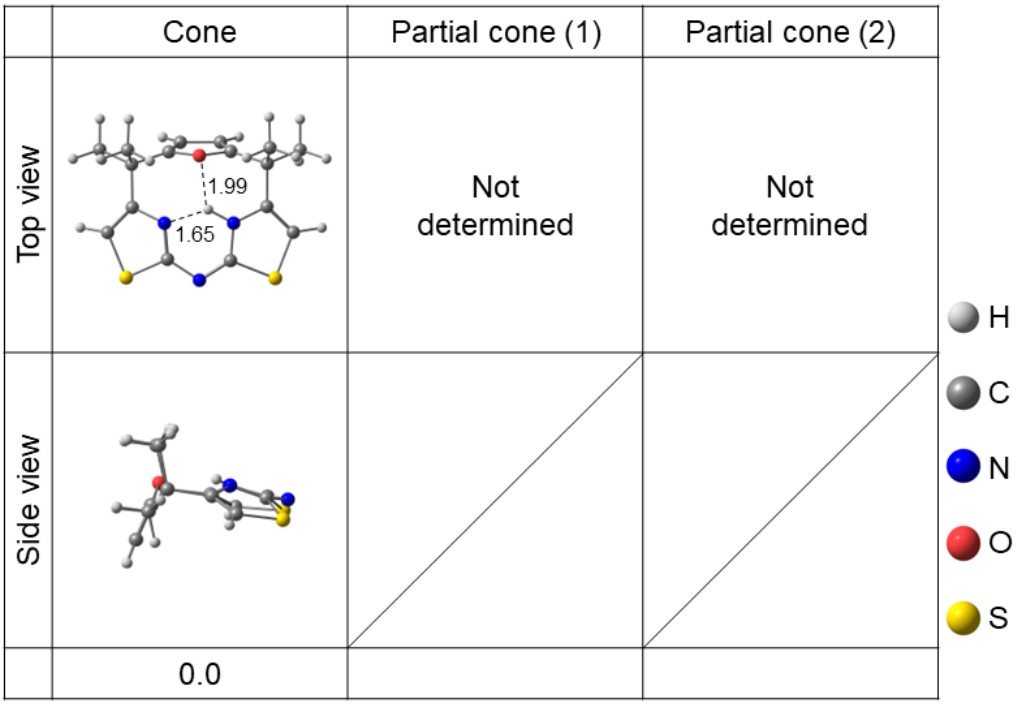

Figure S13. Optimized structures and relative free energies (kcal/mol) for conformers of compound **10**. Selected hydrogen bonding distances (Å) are also shown.

4.3 Relative stability for conformers of compound 3 and 5: DFT functional dependency

(a) Compound **3**

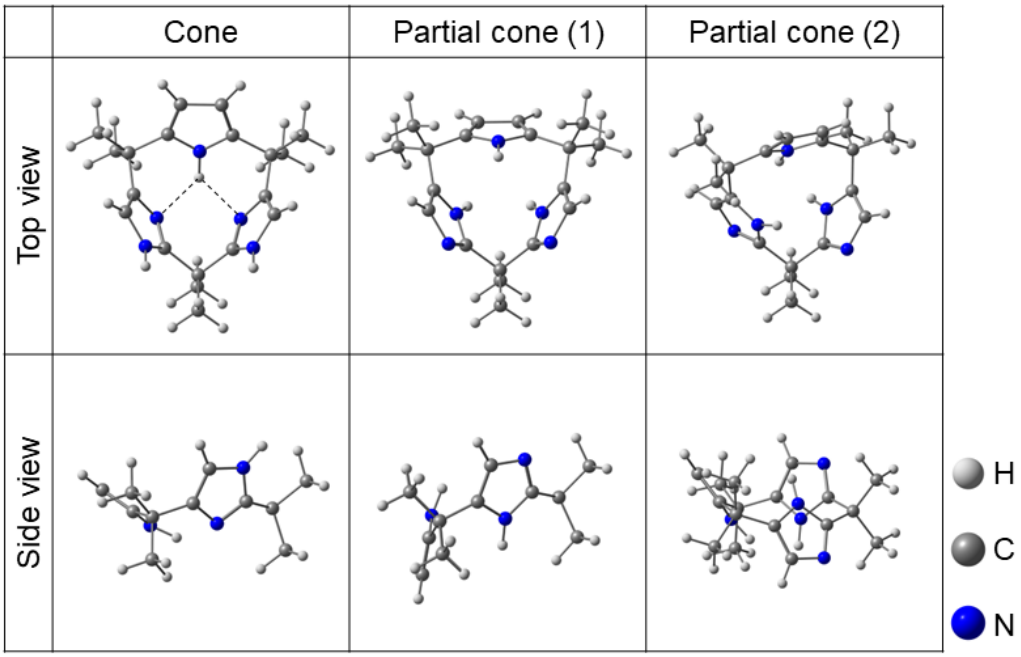

(b) Compound **5**

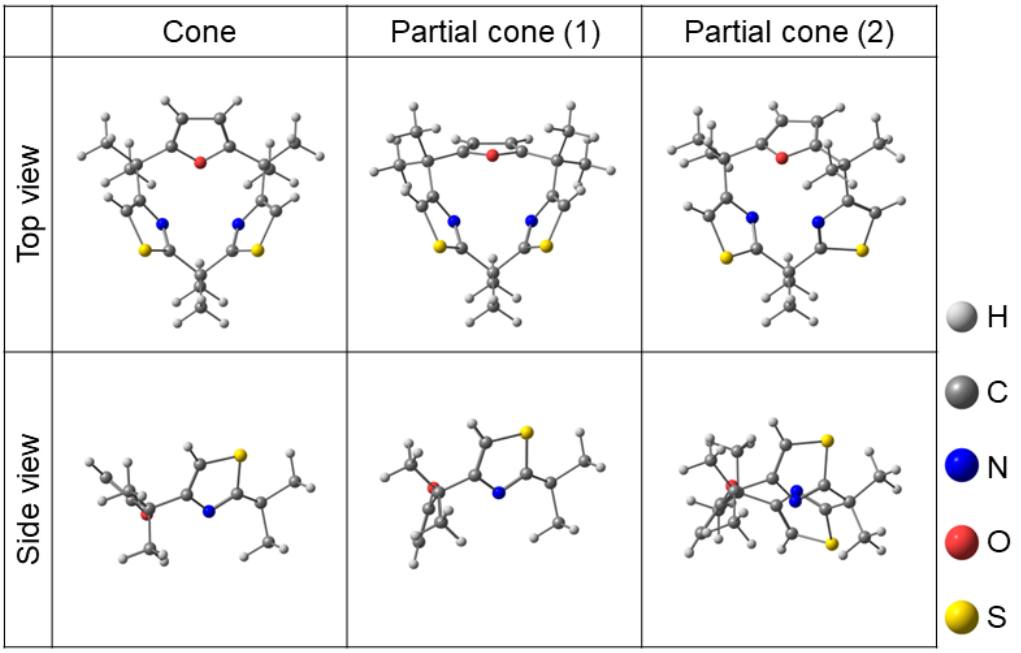

Figure S14. Three conformational structures of compound **3** and **5**.

Table S1. Relative free energies (kcal/mol) for conformers of **3** and **5** at the DFT/6-311+G(2d,p) level of theory.

3	B3LYP+D3	*ω*B97X-D	M06	M06-2X
Cone	0.2	0.9	0.2	0.6
Partial cone (1)	0.7	0.7	0.9	0.7
Partial cone (2)	0.0	0.0	0.0	0.0
5	B3LYP+D3	*ω*B97X-D	M06	M06-2X
Cone	0.2	0.4	1.0	0.4
Partial cone (1)	0.1	0.3	0.2	0.3
Partial cone (2)	0.0	0.0	0.0	0.0

For both compounds, the results at the four representative DFT level of theory show that the partial cone (2) conformer is identified as the lowest energy conformer.

4.4 Fragments used in ring strain estimation by StrainViz

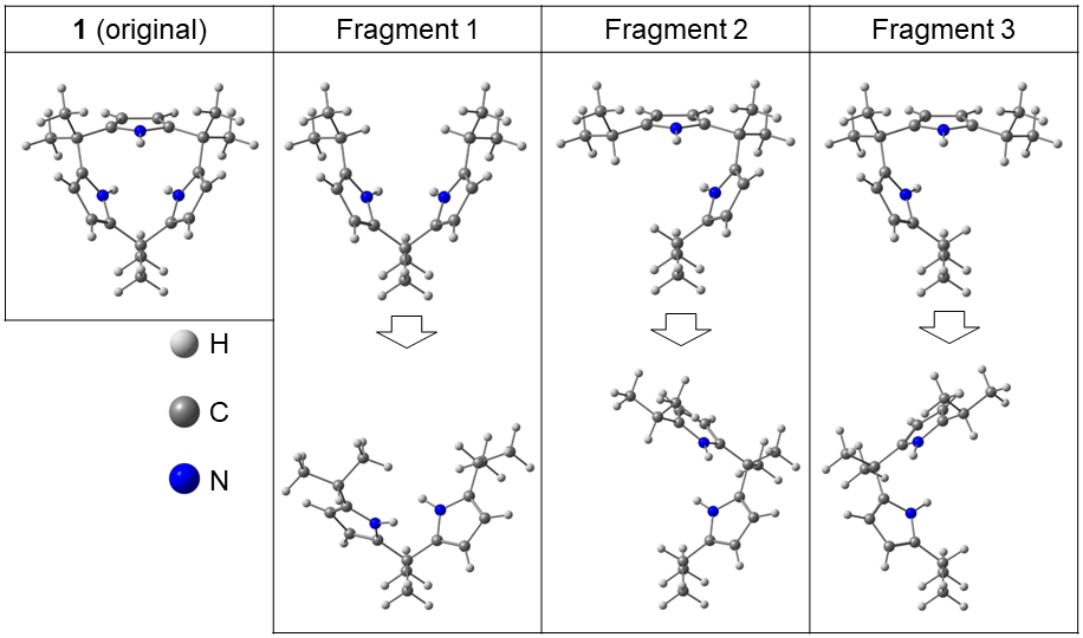

Figure S15. Lowest energy conformer of compound **1**. Initial and optimized structures of fragments used in ring strain evaluation by StrainViz.

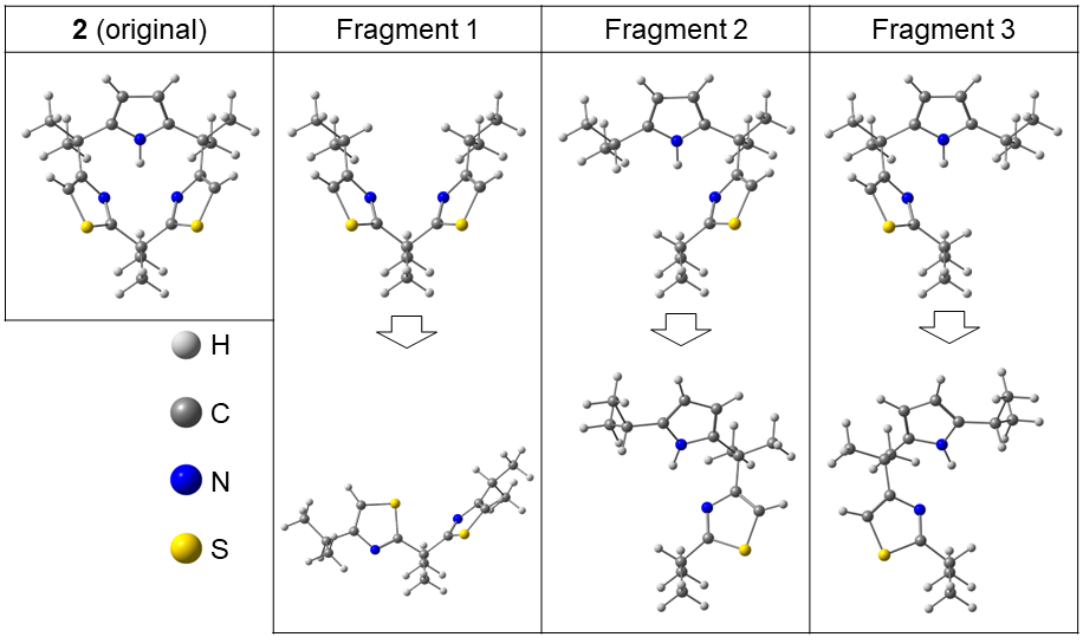

Figure S16. Lowest energy conformer of compound **2**. Initial and optimized structures of fragments used in ring strain evaluation by StrainViz.

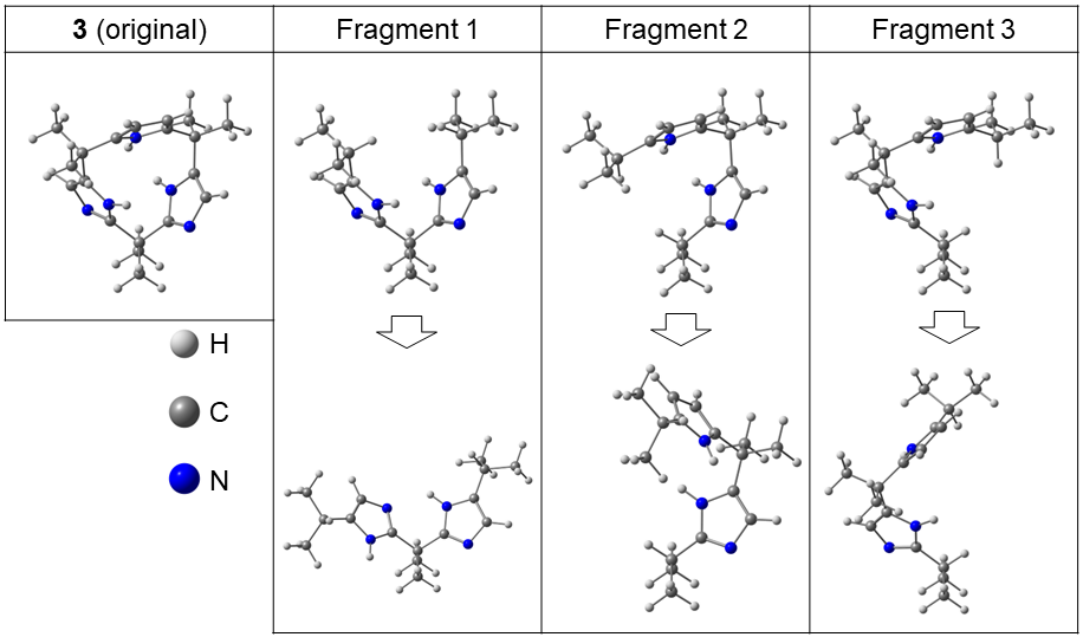

Figure S17. Lowest energy conformer of compound **3**. Initial and optimized structures of fragments used in ring strain evaluation by StrainViz.

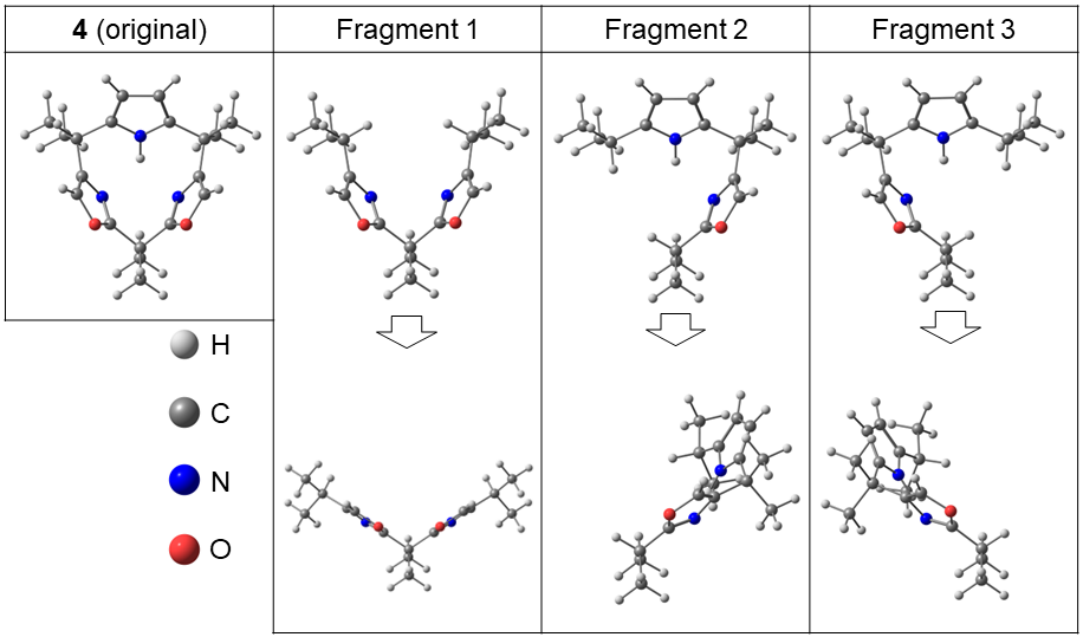

Figure S18. Lowest energy conformer of compound **4**. Initial and optimized structures of fragments used in ring strain evaluation by StrainViz.

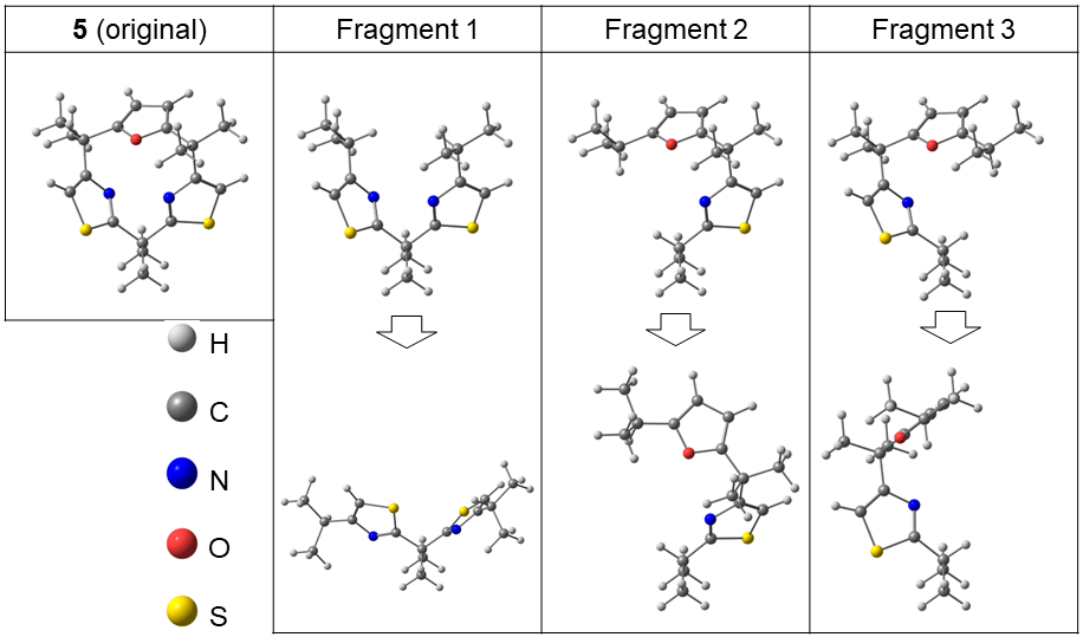

Figure S19. Lowest energy conformer of compound **5**. Initial and optimized structures of fragments used in ring strain evaluation by StrainViz.

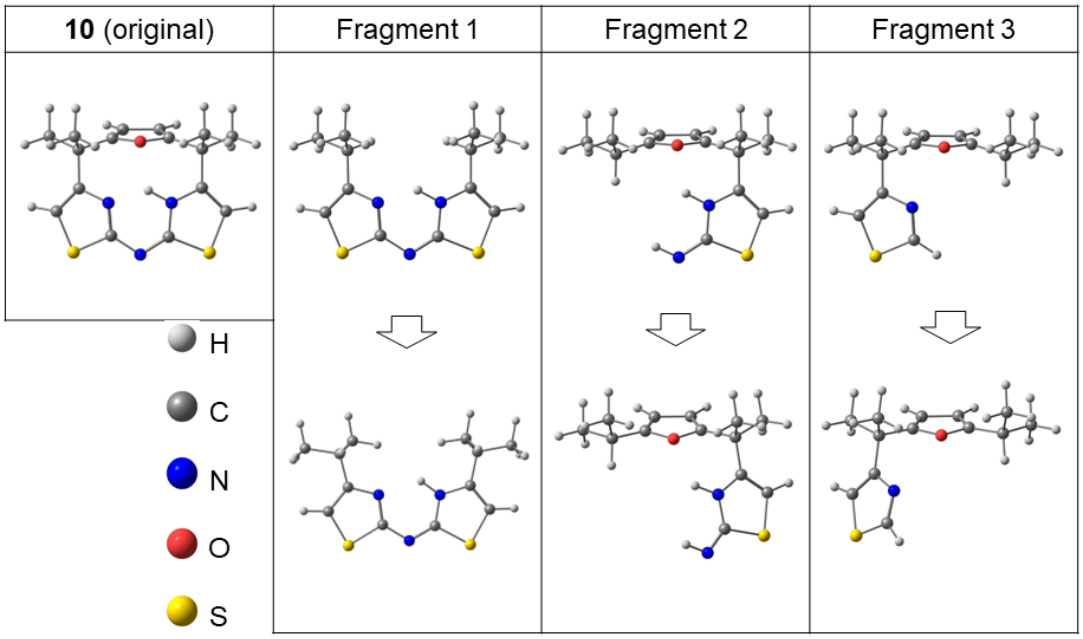

Figure S20. Lowest energy conformer of compound **10**. Initial and optimized structures of fragments used in ring strain evaluation by StrainViz.

4.5 Dihedral strain as major contribution of total strain

Figure 1c shows that the dihedral strain mainly contributes the total one (see main text). As visualized in Figure S15b and c, the distributions of dihedral strain are also similar to the those of total strain.

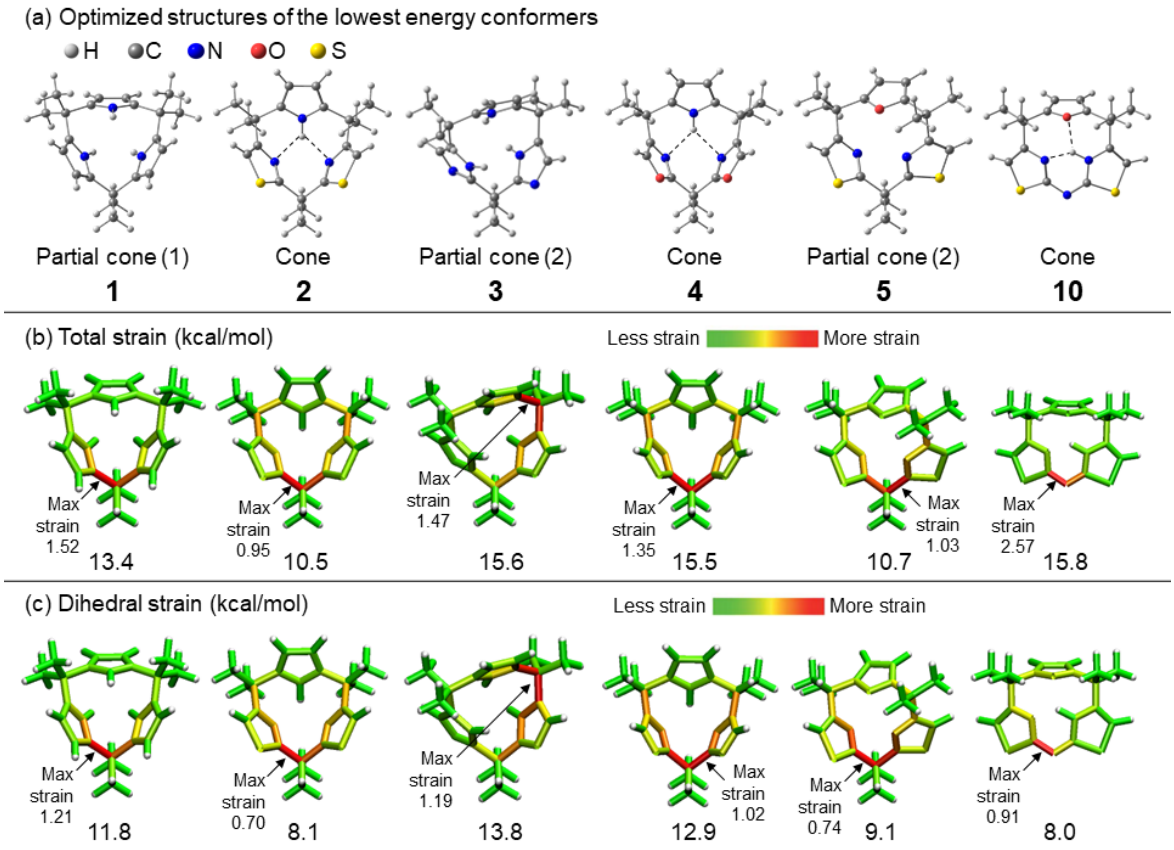

Figure S21. Visualization of total and dihedral strain distributions. In the StrainViz analysis, total strain is evaluated as summed energy of bond, angle, and dihedral strains. Color distribution corresponds to the strain energy range between maximum and minimum values in each case.

4.6 Inner NH proton-dependent ring strain of compound 3

For the partial cone conformers (1) and (2) of **3**, the energy distribution and magnitude of total (dihedral) strain are sensitive to the pairs of 5-membered rings with inner NH proton (marked as asterisk).

Although the partial cone (1) of **3** has the same conformation manner as **1**, the distribution and maximum value of total (dihedral) strain of **3** are different from those of **1**.

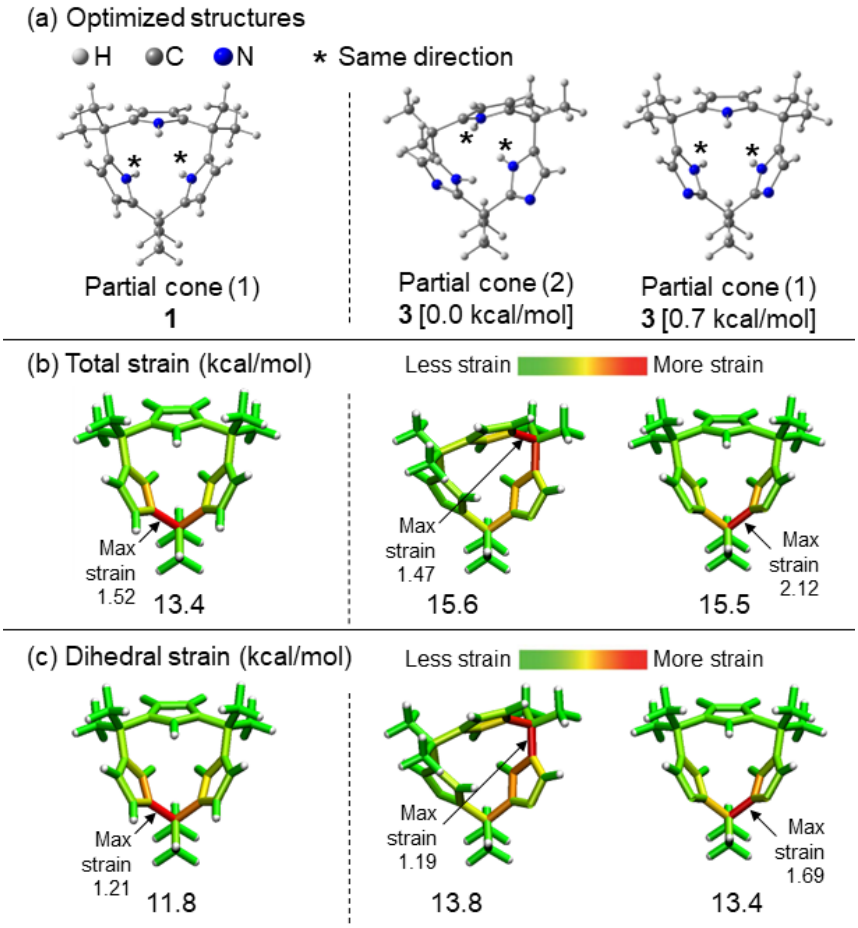

Figure S22. Visualization of total and dihedral strain distributions of **3** with two partial cone types. In the StrainViz analysis, total strain is evaluated as summed energy of bond, angle, and dihedral strains. The results of **1** are shown for comparison. Color distribution corresponds to the strain energy range between maximum and minimum values in each case.

4.7 Evaluation of ring strain at different computational level

The ring strain at the B3LYP/6-311+G(2d,p) level of theory was calculated for comparison. Figure S17 shows the evaluation of ring strain and visualization of energy distribution for the selected compounds (**1**, **2**, and **4**). From the total and dihedral strains, it is found that **2** exhibits less strain rather than **1** and **4**, in agreement with the M06-2X results in Figure 1 (see the main text). The energy distributions are also similar to those with the M06-2X functional in Figure S15. Thus, there is no influence of the selected different computational level for the ring strain analysis.

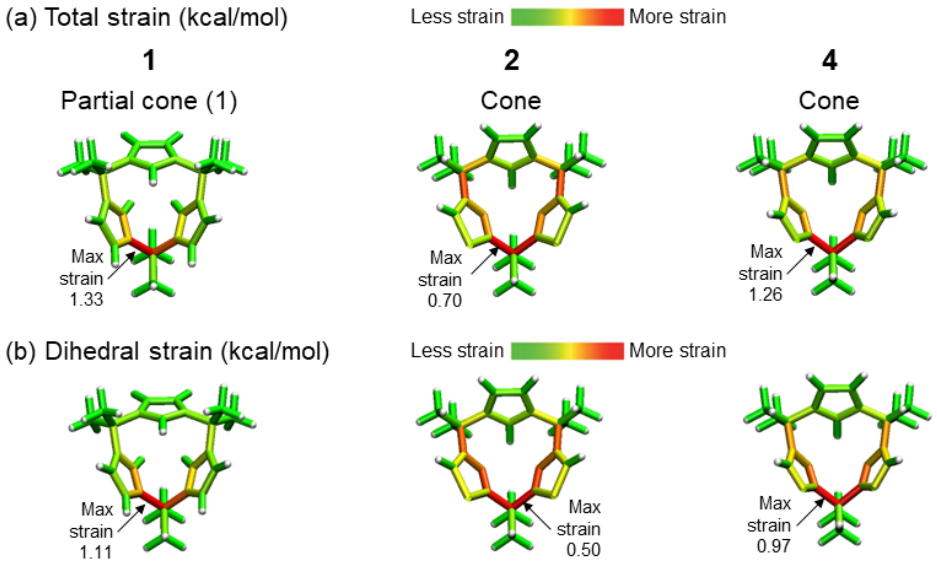

(c)

Compound	1	2	4
Total strain	12.7	9.0	14.4
Bond strain	0.5	0.6	0.7
Angle strain	0.9	1.3	1.5
Dihedral strain	11.3	7.2	12.2

(energy in kcal/mol)

Figure S23. Ring strain analysis for **1**, **2**, and **4** calculated at the B3LYP+D3/6-311+G(2d,p) level of theory. (a and b) Visualization of total and dihedral strains. Color distribution corresponds to the strain energy range between maximum and minimum values in each case. (c) Total, bond, angle, and dihedral strains. These structural data are summarized in the section 9 (B).

4.8 Visualization of non-covalent interaction of Pd complex 12

The NCIPLOT result shows the weakly attractive interactions (green colored regions) by hydrogen bonding and anion···π between the Pd complex and counter anions.

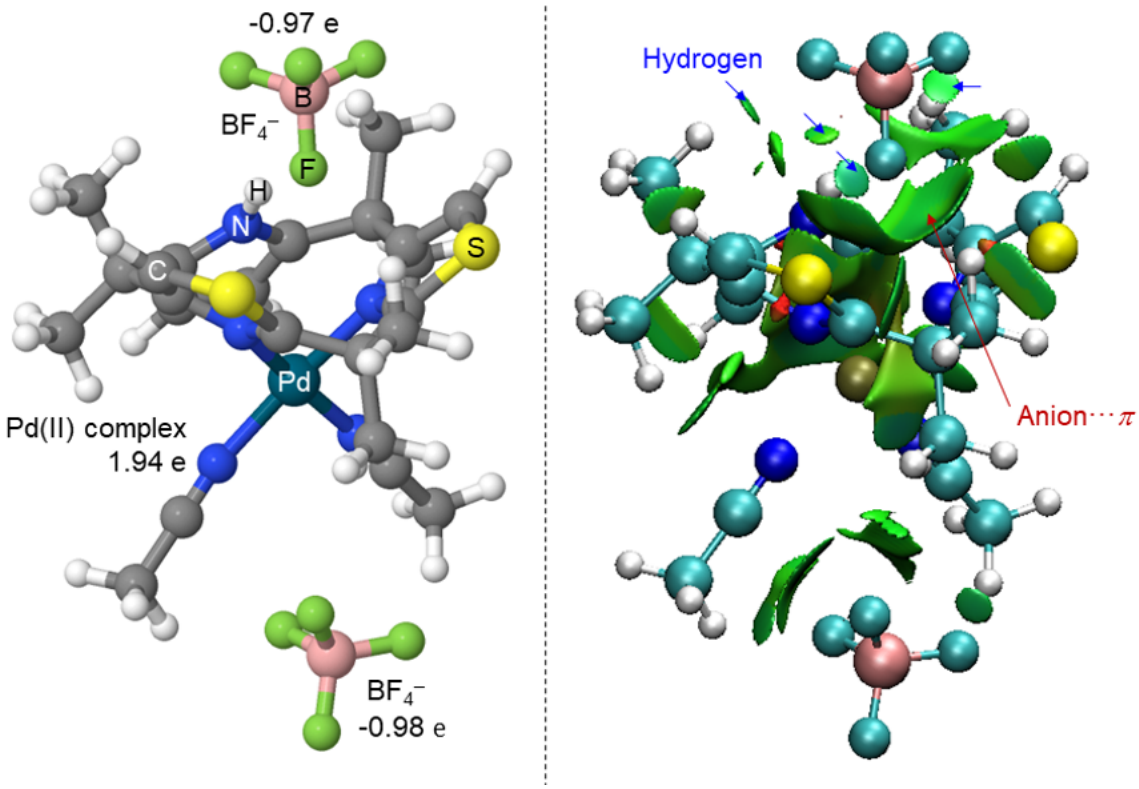

Figure S24. Visualization of non-covalent interaction of Pd complex **12**. Charges of Pd complex and BF_4 are assigned from the natural charges by the NBO analysis.

5. Comparison of Ring-size Selectivity

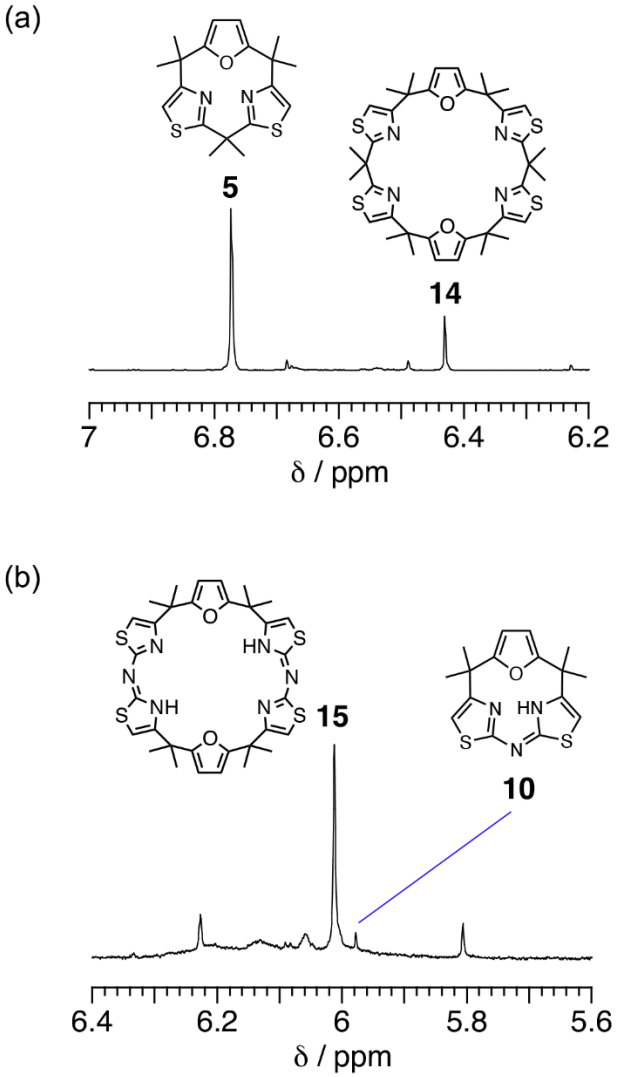

Figure S25. ^{1}H NMR spectra (400 MHz, $CDCl_3$) of crude reaction mixtures of the direct macrocyclization synthesis of (a) **5** and **14**, and (b) **15** and **10**.

6. Ring Opening Polymerization of *rac*-lactide

Polymerization of *rac*-lactide catalyzed by Zn complex **11**

Complex **11** (18 mg, 40 μmol) and *rac*-lactide (288 mg, 2.0 mmol) were placed in a 10 mL Schlenk-tube under N_2 atmosphere. A 40 mM toluene solution of benzyl alcohol (1.0 mL) was added to dissolve the solid materials, and the resulting solution was stirred for 30 min at 120 °C. After cooling the mixture to room temperature, the reaction was quenched with methanol (8.0 mL). The precipitate formed was collected by filtration, and washed with small amount of methanol to give polylactic acid as a white solid (96% conversion).

HPLC analysis

The molecular weight values (M_n, M_w) were determined by gel permeation chromatography calibrated with polystyrene standards in THF. The polystyrene standards set used for calibration was purchased from Agilent (PS-L (162-50,000)). The calibration curve was represented as

$$\log \mathrm{M} = 9.867 + (-0.5678)\mathrm{tR}$$

M_n, M_w, PDI values were calculated as 9.045 kg/mol, 12.78 kg/mol, 1.413 respectively.

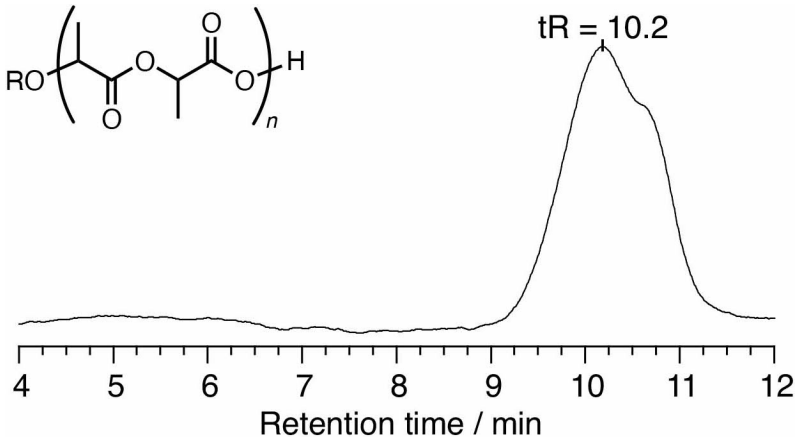

Figure S26. HPLC chromatogram of the obtained poly lactic acid (Column: Shodex KF-804L, mobile phase: tetrahydrofuran, detection: Reflection Index; flow rate: 1.0 mL/min.).

7. Metal Complexation Study Using NMR Spectroscopy

7.1 Stability tests of Zn complex 11

General procedures for stability tests

Stability tests were performed using ^{1}H NMR spectroscopy. An NMR tube was charged with 0.5 mL of $CDCl_3$ solution of **11** (13.3 mM), and then a certain amount of substrate was added. After the fixed interval, the recovery rate of complex **11** was calculated using the $CHCl_3$ signal as an internal standard.

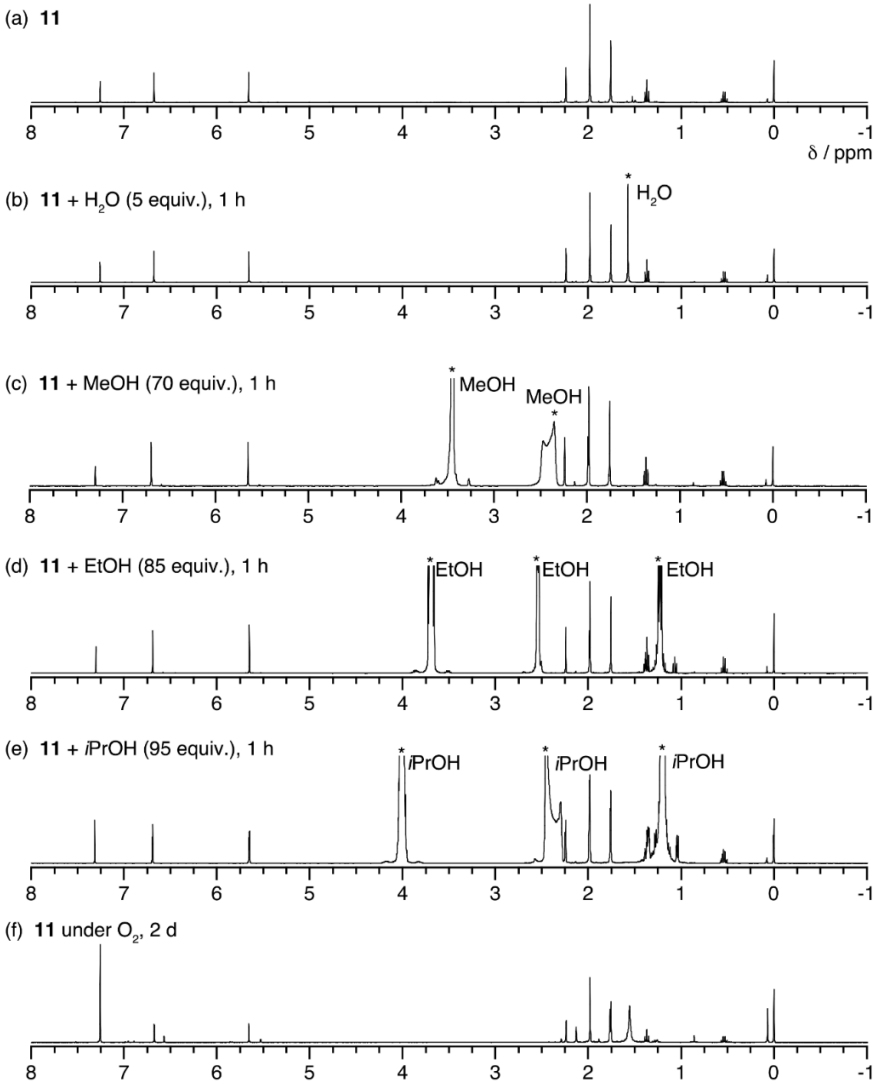

Figure S27. ^{1}H NMR spectra (400 MHz, $CDCl_3$) of (a) the test solution of **11** (before addition of substrate), 1 h after addition of (b) water (5 equiv.), (c) methanol (70 equiv.), (d) ethanol (85 equiv.), (e) *i*-PrOH (95 equiv.), and (f) after 2 d under O_2 atmosphere.

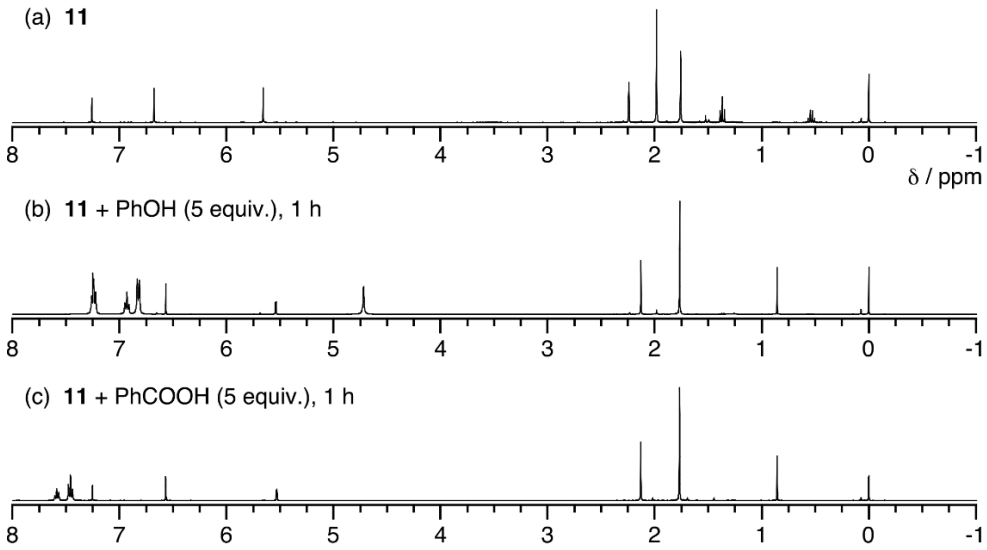

Figure S28. ^{1}H NMR spectra (400 MHz, $CDCl_3$) of (a) the test solution of **11** (before addition of substrate), 1 h after addition of (b) phenol (5 equiv.), (c) benzoic acid (5 equiv.)

7.2 Complexation behavior of ligand 2 with Pd^{2+} ions

For metal complexation study of **2** with Pd was performed in CD_3CN at 298 K. ^1H NMR spectral titration experiment was conducted by adding a solution of tetrakis(acetonitrile)palladium(II) tetrafluoroborate (0.1 M in CD_3CN) into a solution of calix[1]pyrrole[2]thiazole **2** (5.6 mM in CD_3CN) in an NMR tube.

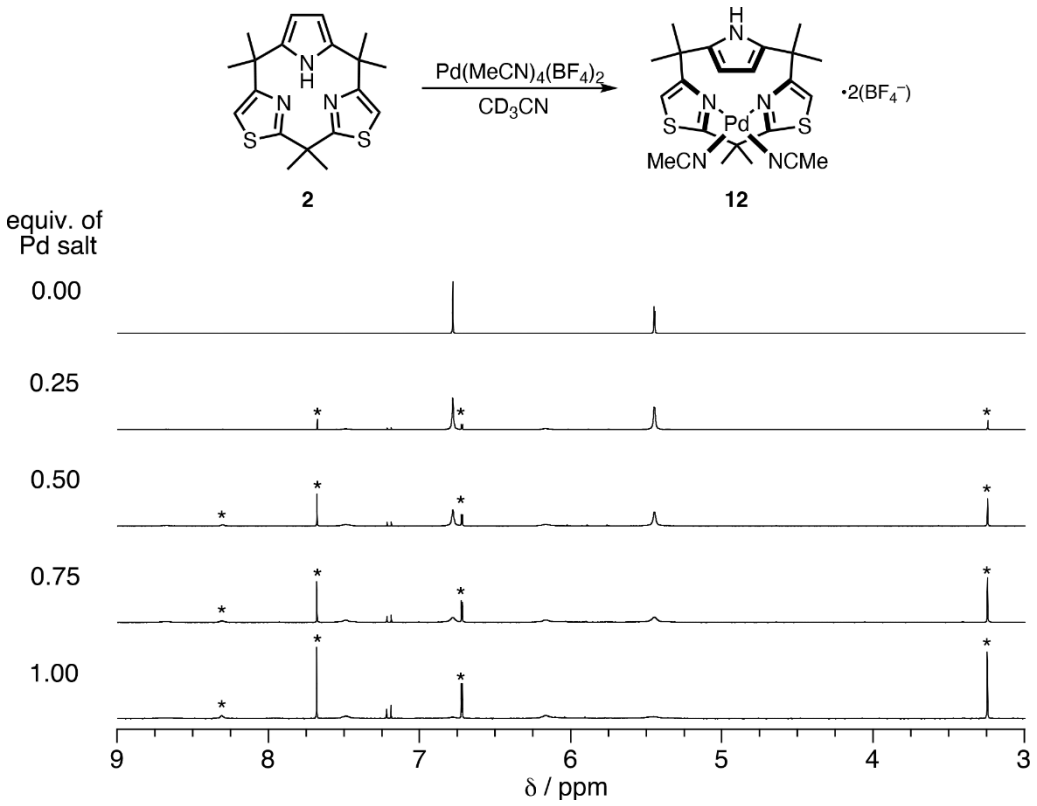

Figure S29. 400 MHz ^1H NMR spectra of compound **2** in CD_3CN at 5.6 mM (from top to bottom) before and after the addition of tetrakis(acetonitrile)palladium(II) tetrafluoroborate (from 0.25 to 1.00 equiv.). Asterisks indicate proton signals from complex **12**.

7.3 NMR titration of 2 with Ag^+ ions

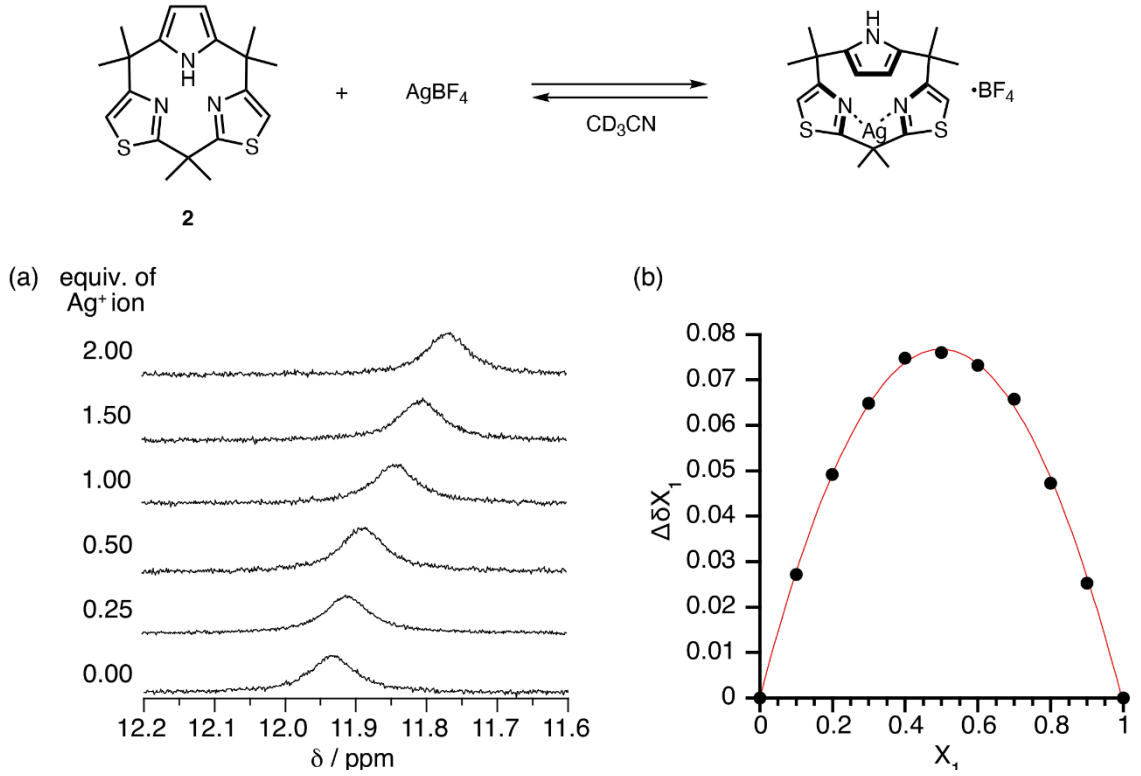

Figure S30. (a) ^{1}H NMR spectra (400 MHz) of compound **2** in CD_3CN (5.6 mM) in the presence of 0, 0.25, 0.50, 1.00, 1.50 and 2.00 equiv of $AgBF_4$. (b) Job's plot analysis for complexation between **2** and Ag^+ ion at [**2**] + [$AgBF_4$] = 20 mM, X_1 = [**2**]/([**2**]+[$AgBF_4$]).

8. Experimental Spectra of New Compounds

8.1 ^{1}H NMR spectra of protonation behavior of 5

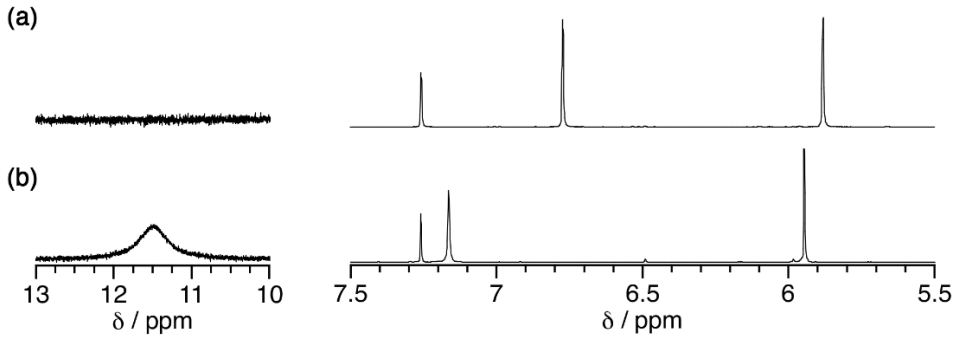

Figure S31. ^{1}H NMR spectra (400 MHz, 298 K, $CDCl_3$) of (a) neutral **5** and (b) **5** with 1.0 equiv. of trifluoroacetic acid.

8.2 UV–vis absorption spectra

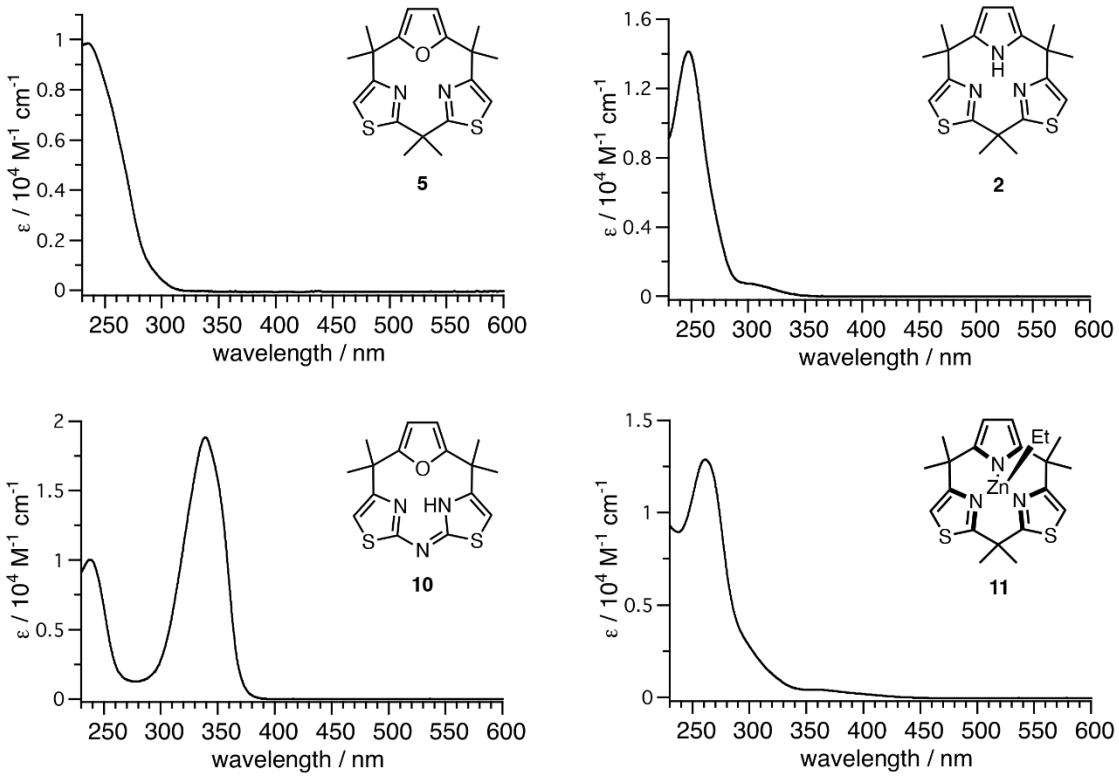

Figure S32. UV–vis absorption spectra of compound **5**, **2**, **10** and **11** in CH_2Cl_2.

8.3 High resolution mass spectra

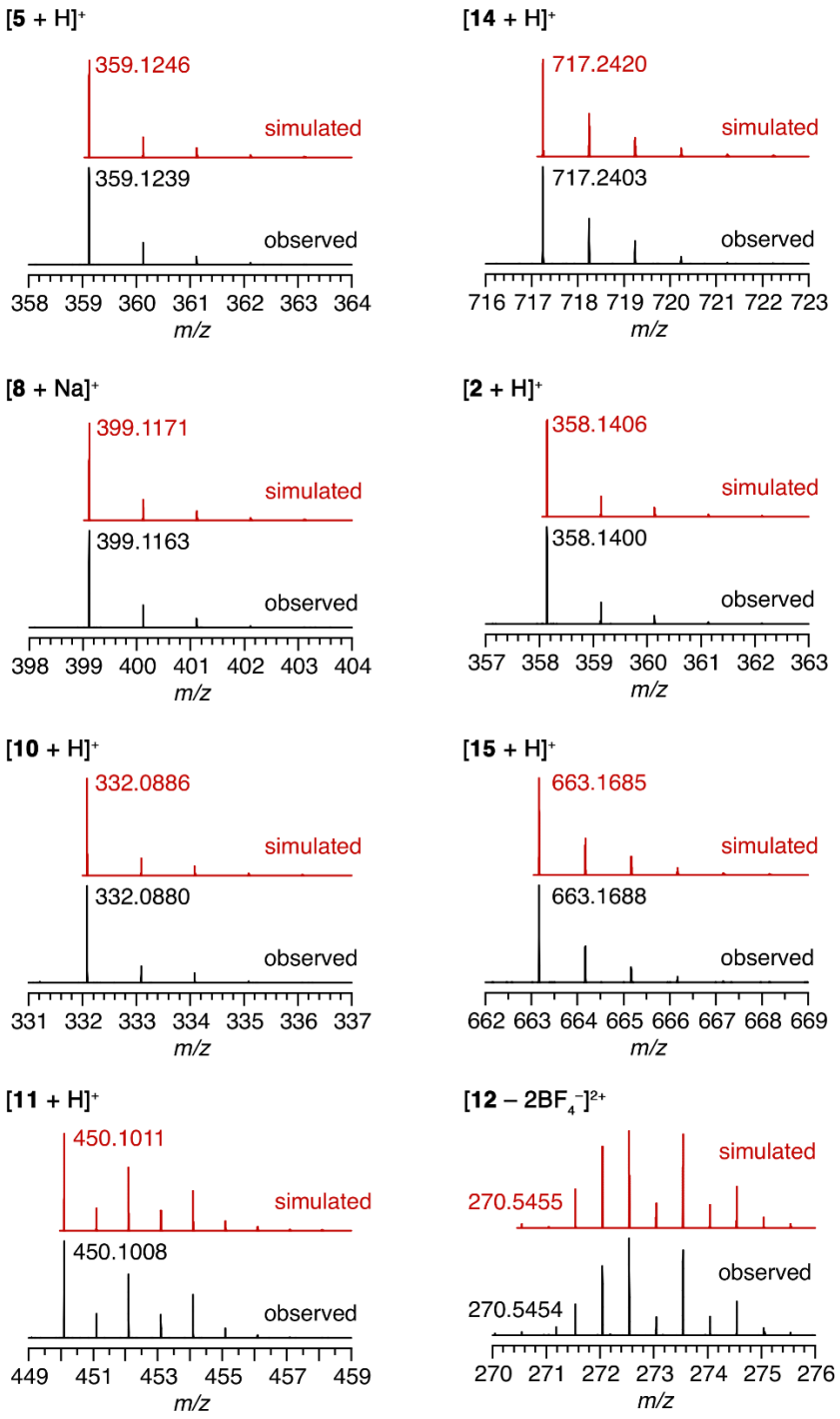

Figure S33. High resolution mass spectra of new compounds. (mobile phase: methanol, positive mode)

8.4 NMR spectra

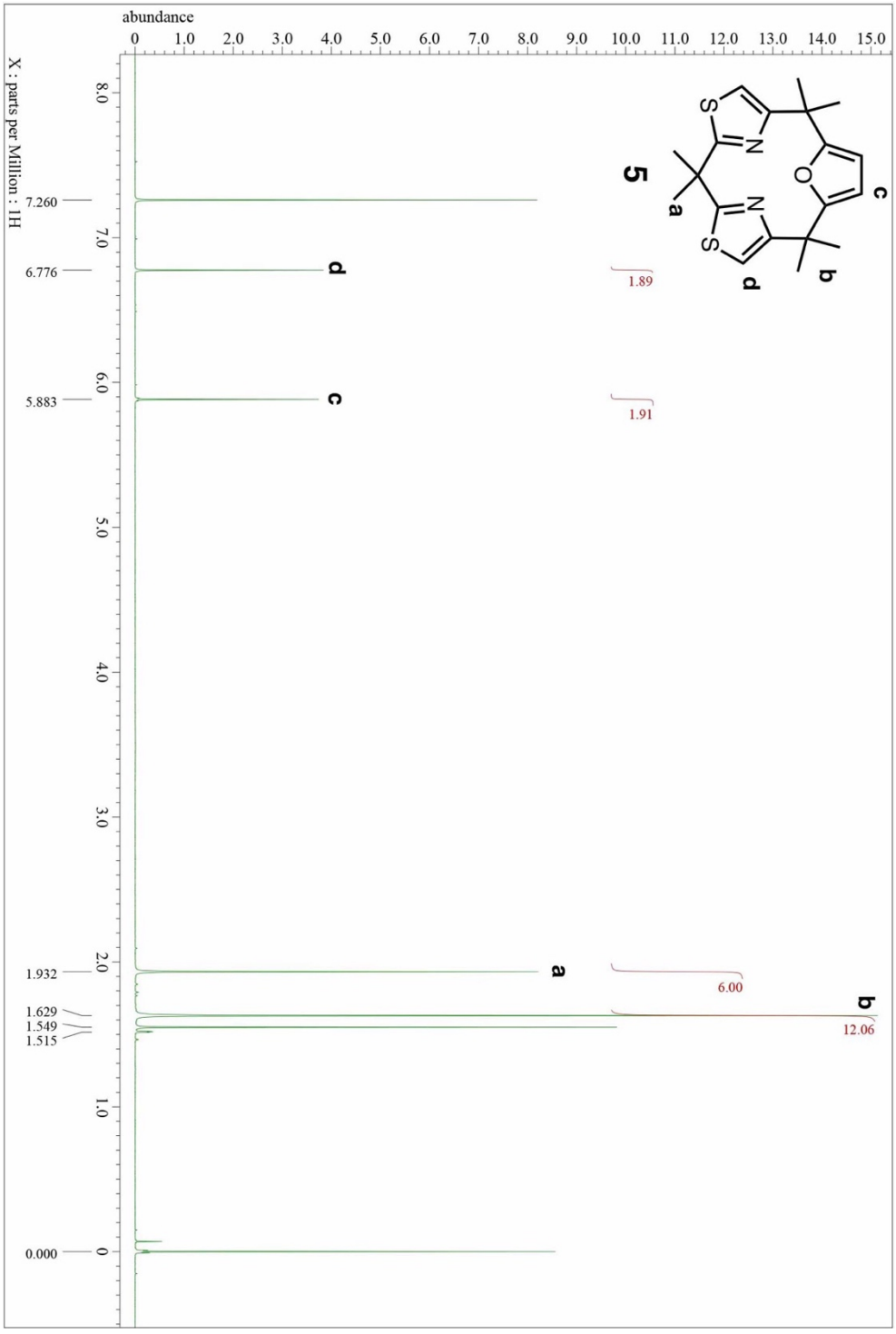

Figure S34. ^{1}H NMR spectrum of compound **5** (400 MHz, $CDCl_3$, 298 K).

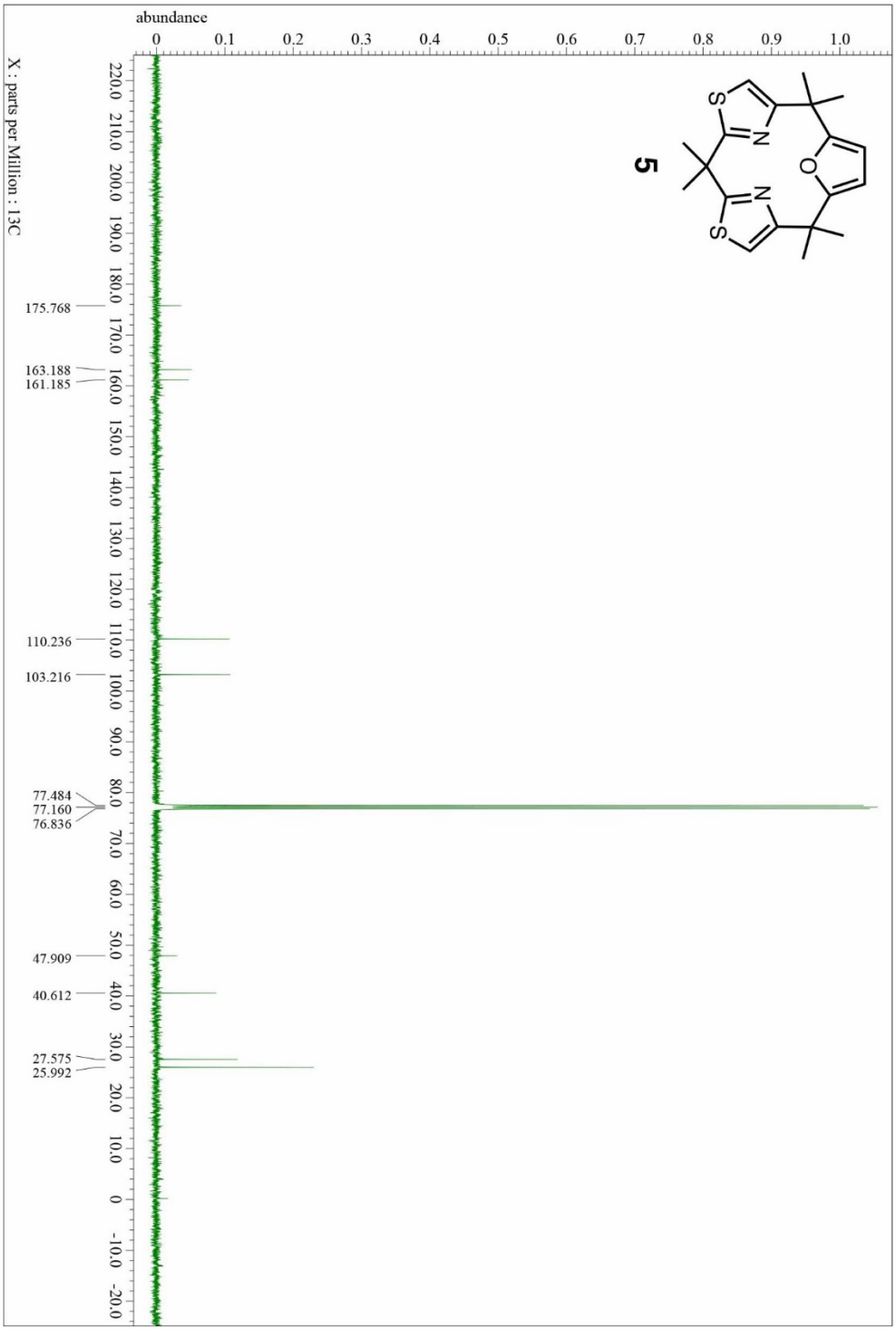

Figure S35. ^{13}C NMR spectrum of compound **5** (100 MHz, $CDCl_3$, 298 K).

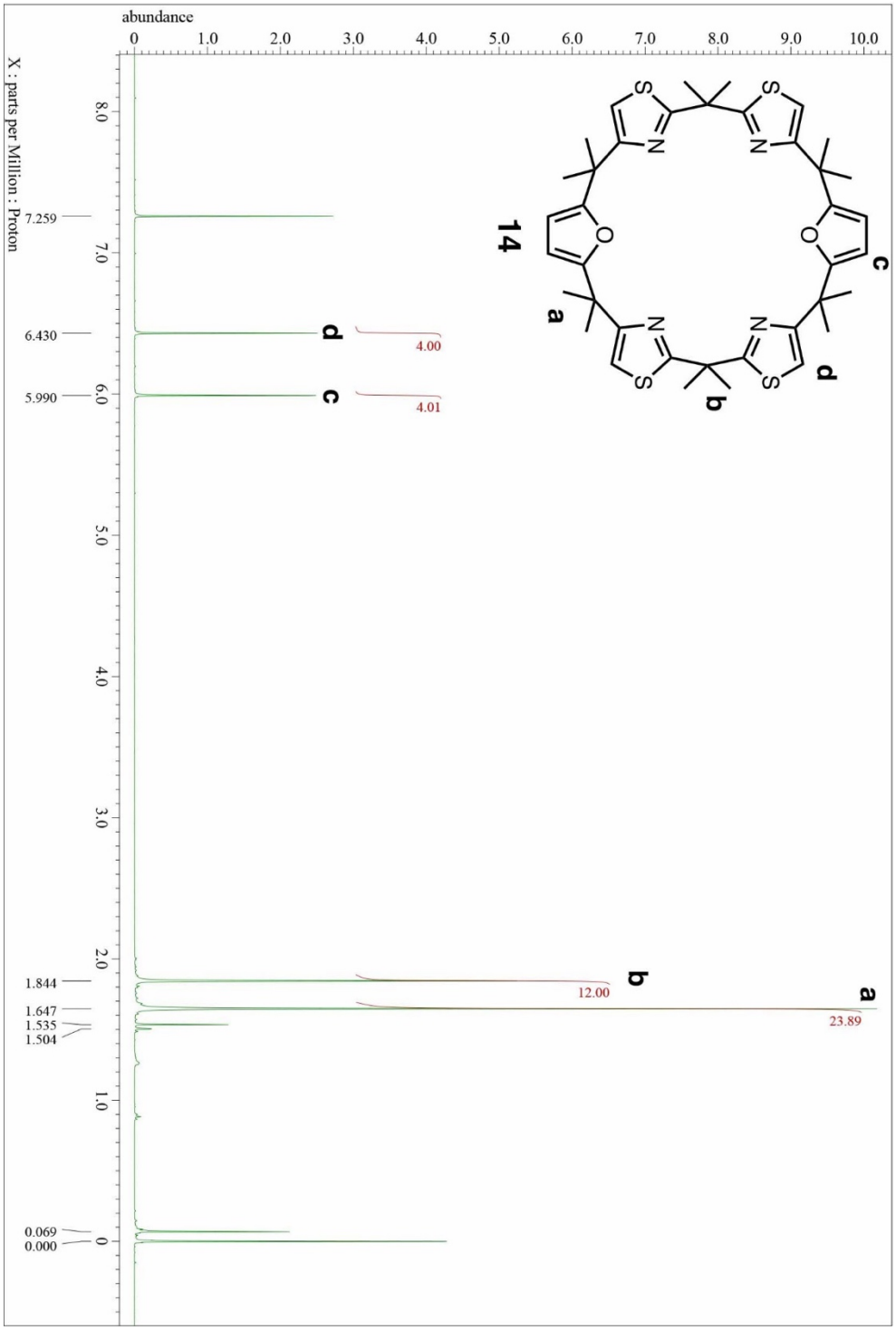

Figure S36. ^{1}H NMR spectrum of compound **14** (400 MHz, $CDCl_3$, 298 K).

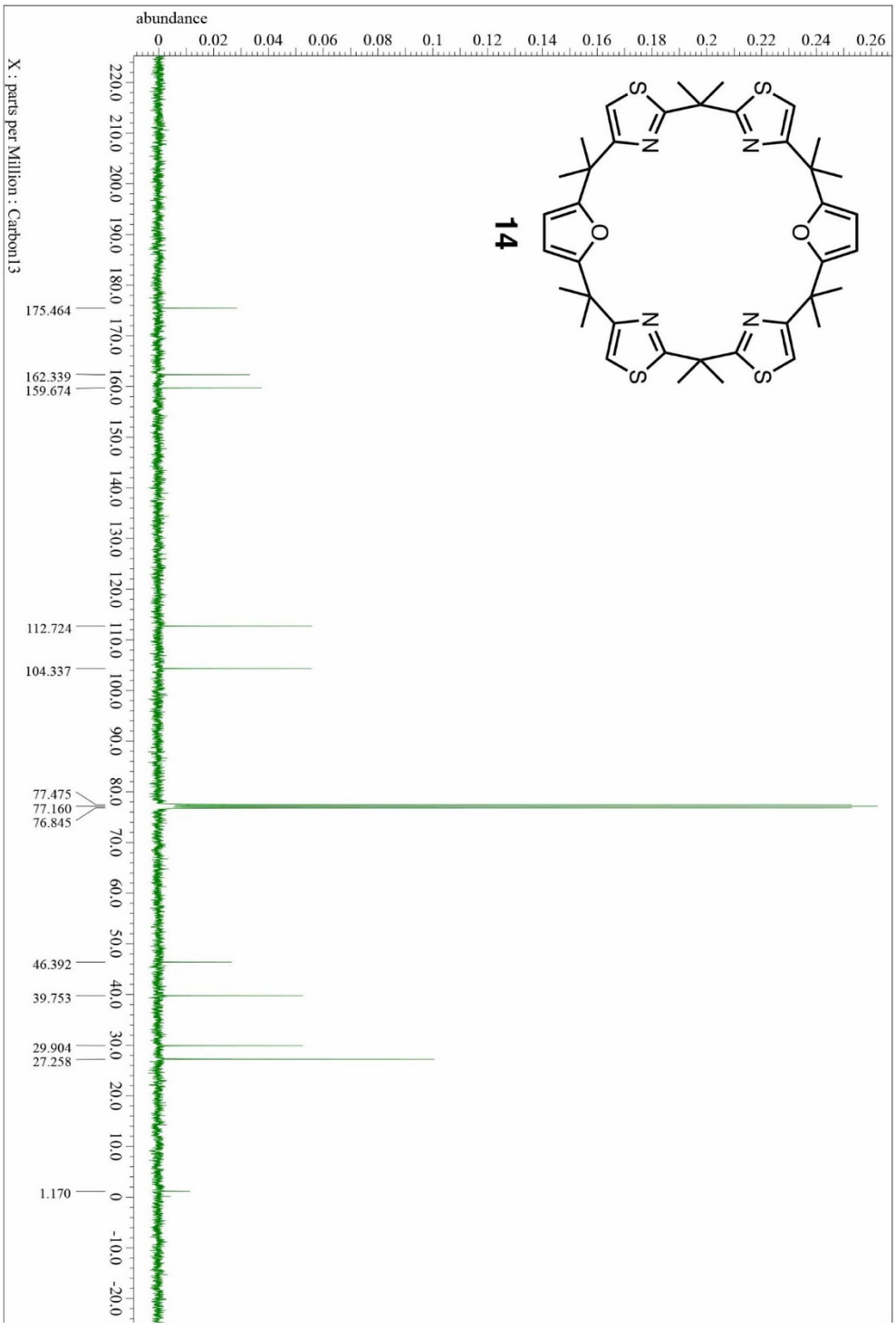

Figure S37. ^{13}C NMR spectrum of compound **14** (100 MHz, $CDCl_3$, 298 K).

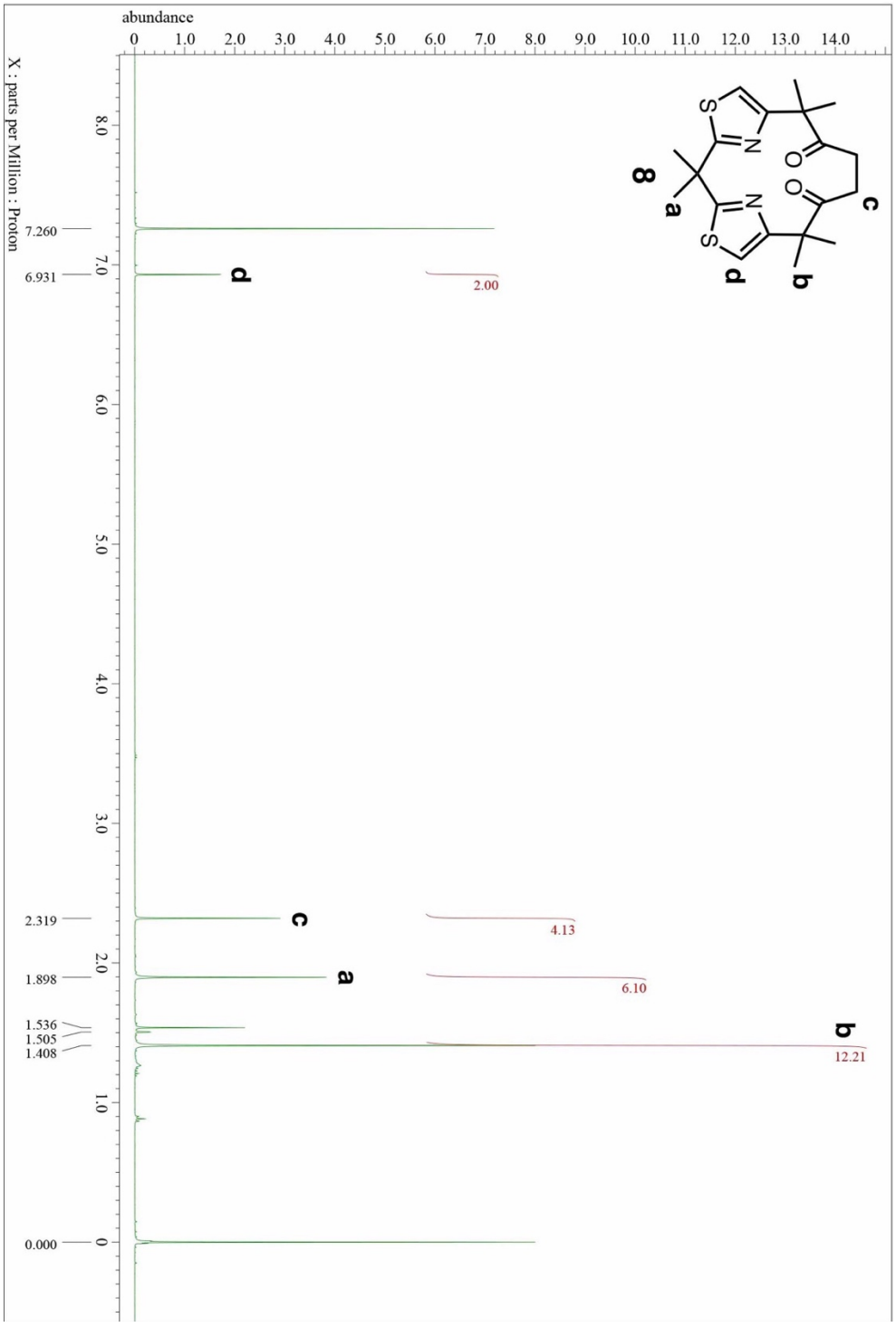

Figure S38. ^{1}H NMR spectrum of compound **8** (400 MHz, $CDCl_3$, 298 K).

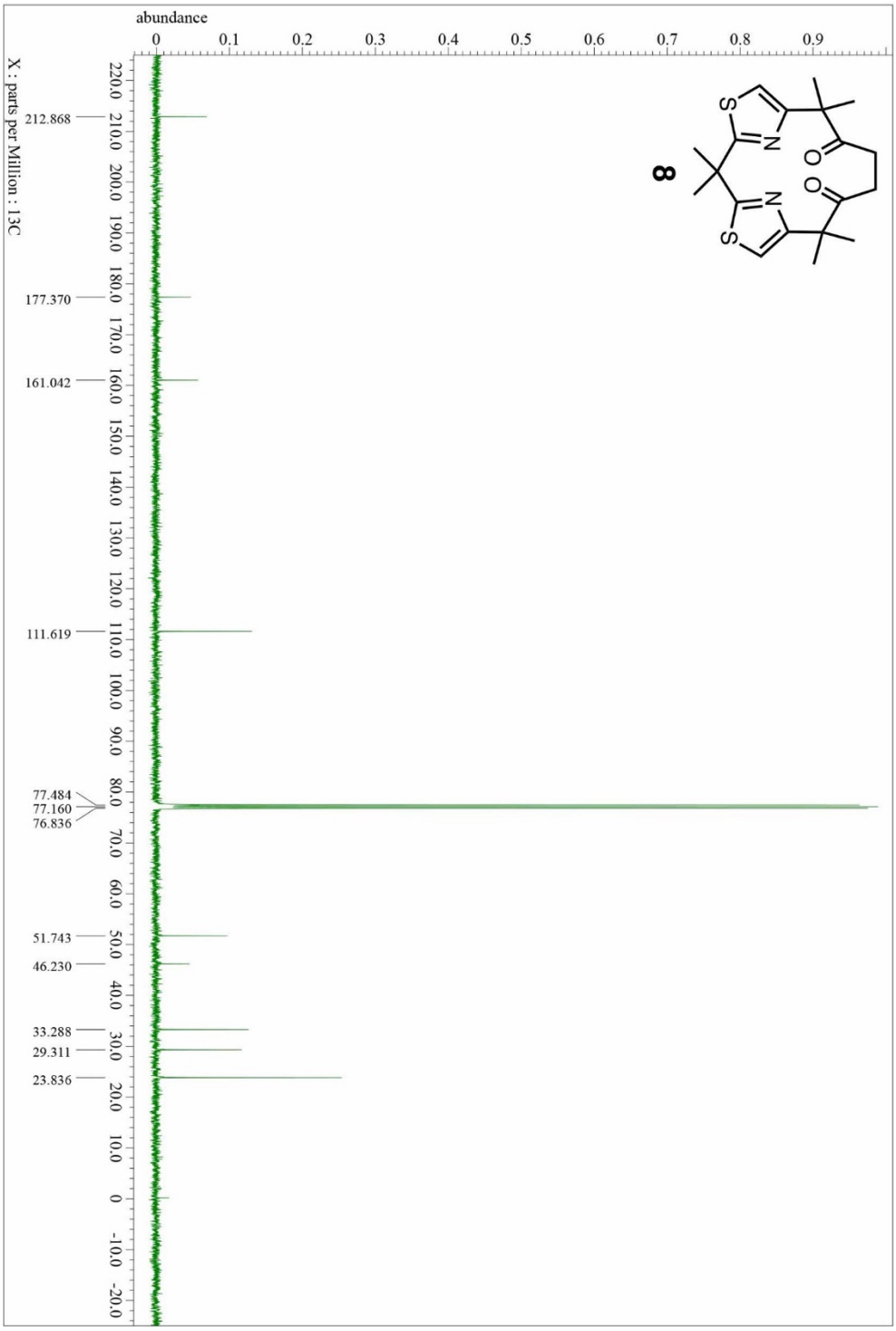

Figure S39. ^{13}C NMR spectrum of compound **8** (100 MHz, $CDCl_3$, 298 K).

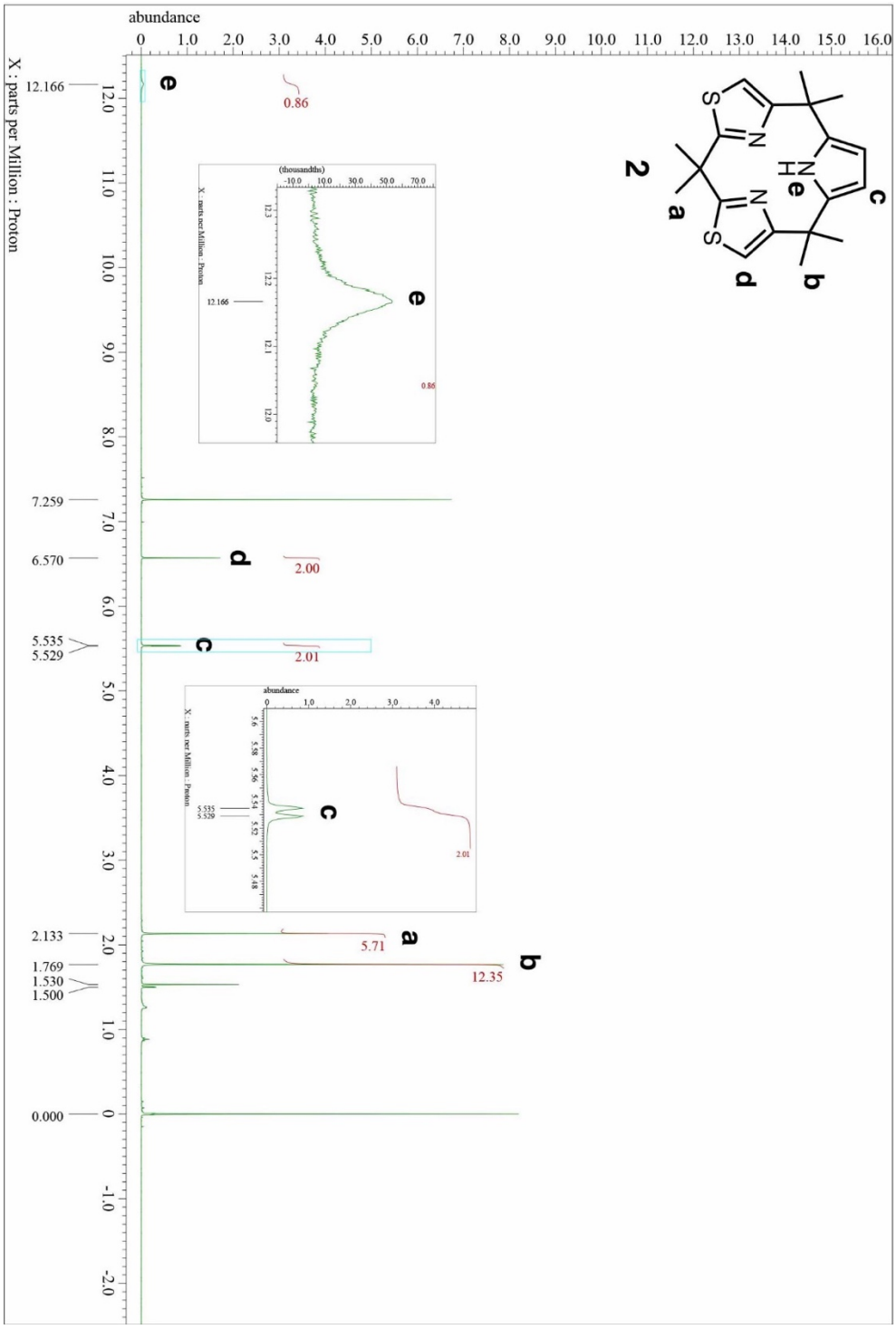

Figure S40. ^{1}H NMR spectrum of compound **2** (400 MHz, $CDCl_3$, 298 K).

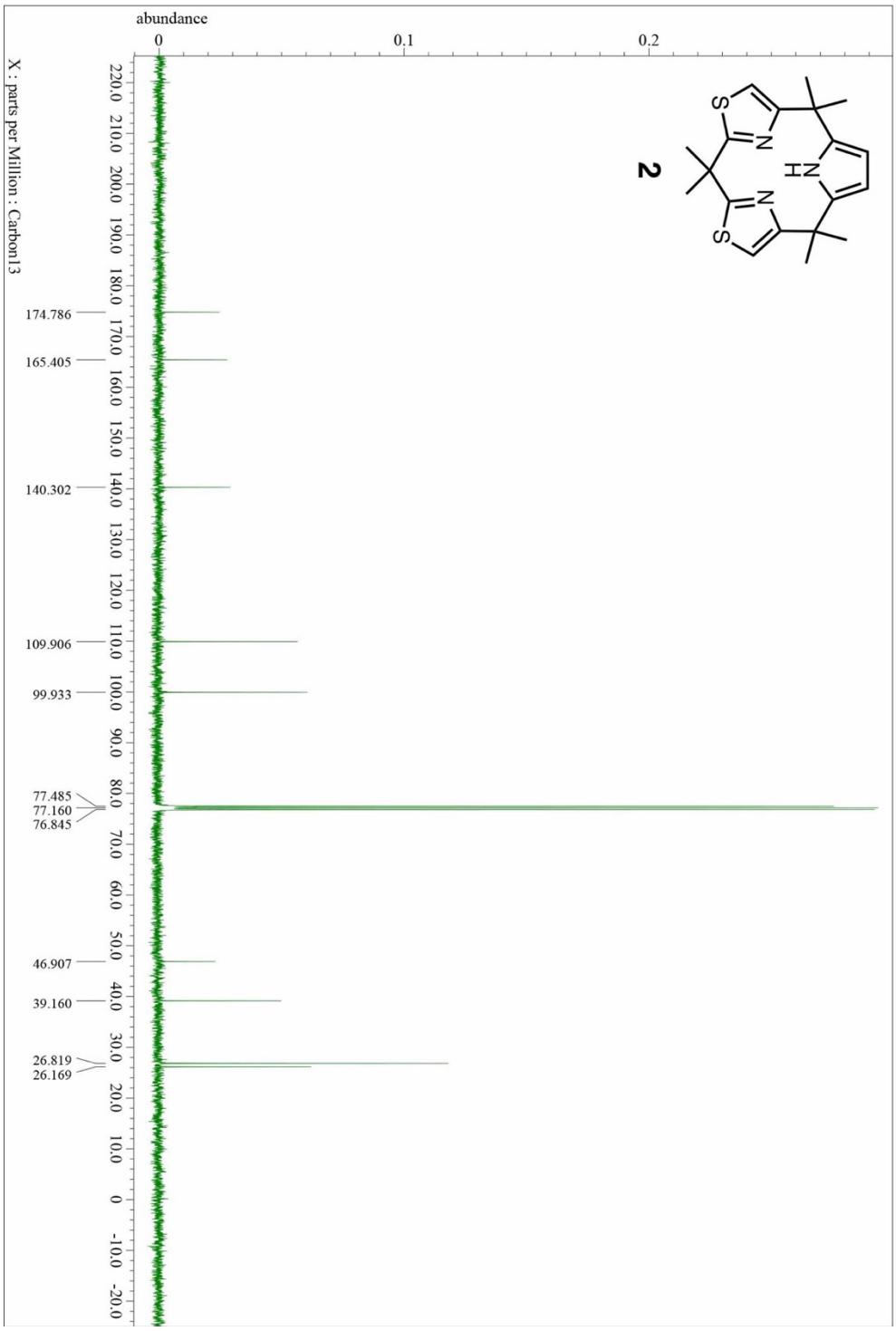

Figure S41. ^{13}C NMR spectrum of compound **2** (100 MHz, $CDCl_3$, 298 K).

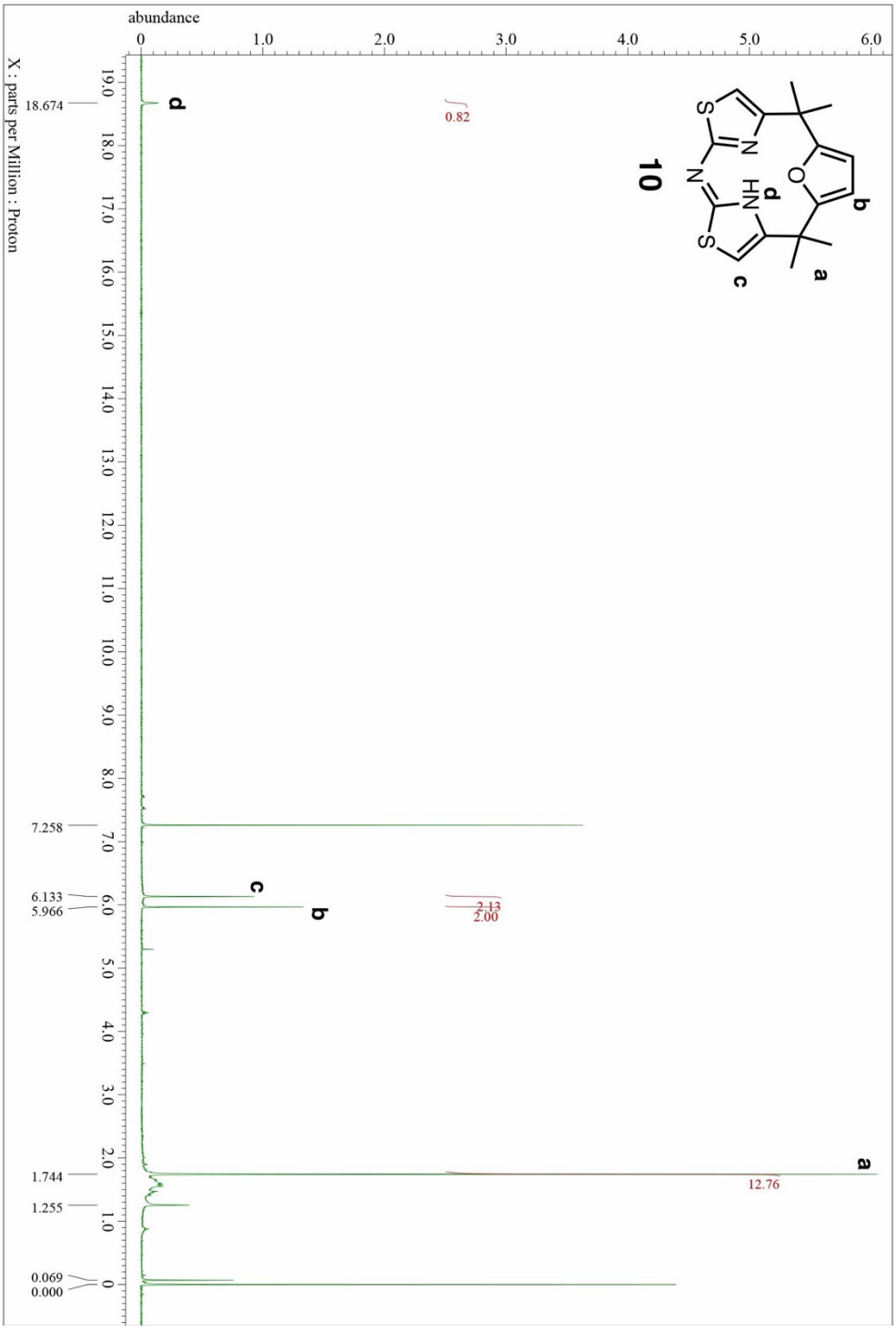

Figure S42. ^{1}H NMR spectrum of compound **10** (400 MHz, $CDCl_3$, 298 K).

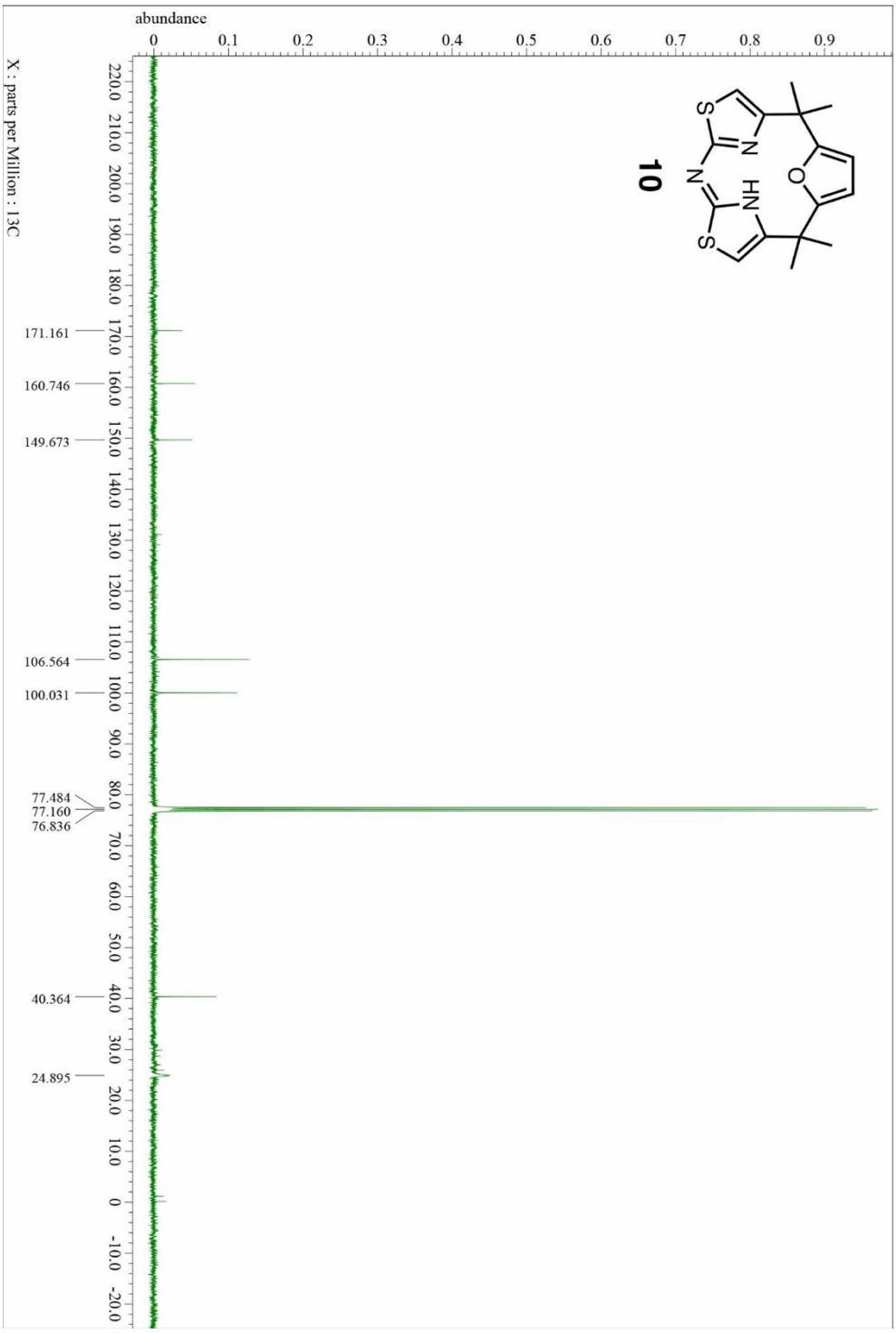

Figure S43. ^{13}C NMR spectrum of compound **10** (100 MHz, $CDCl_3$, 298 K).

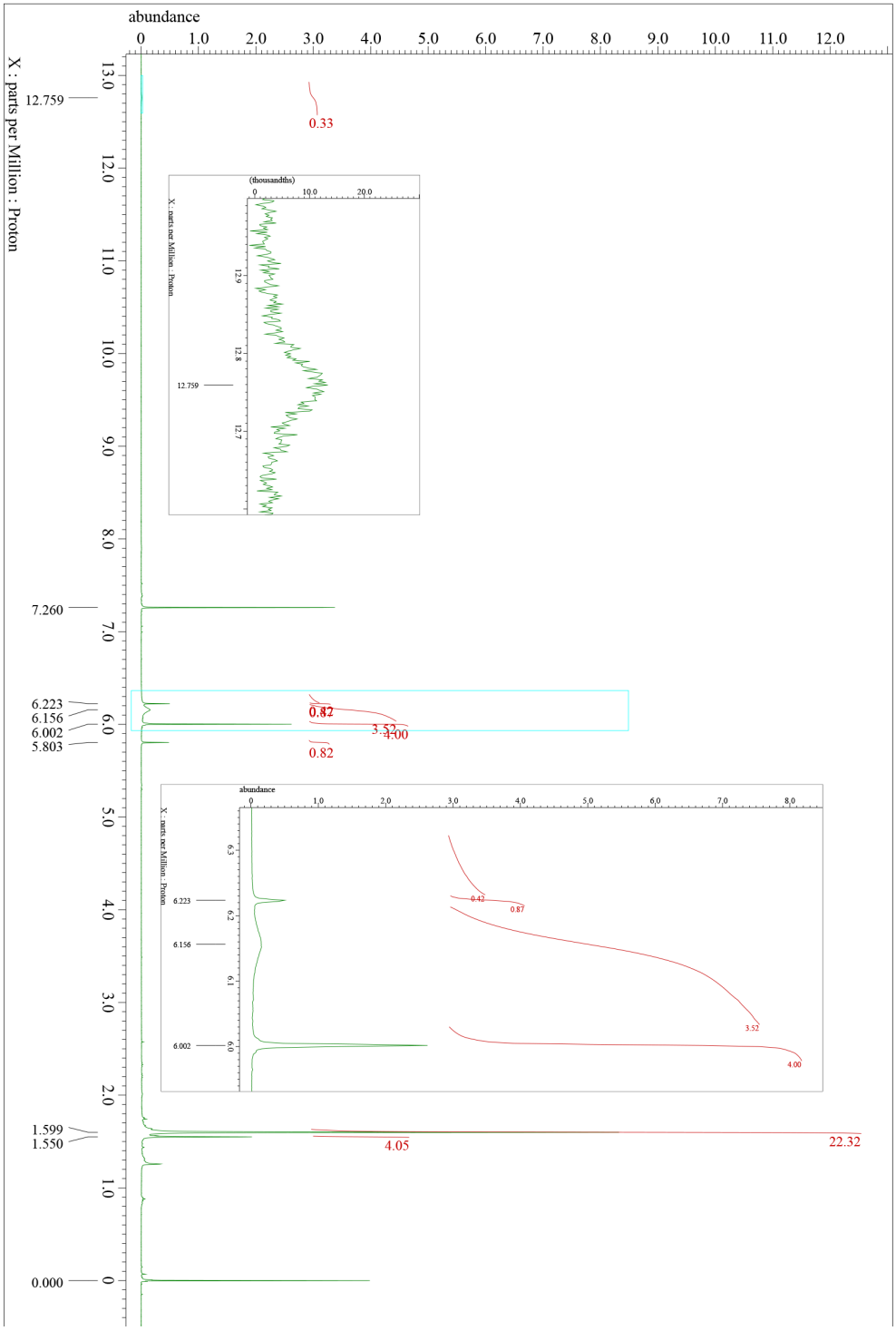

Figure S44. ^{1}H NMR spectrum of compound **15** containing major and minor tautomers (400 MHz, $CDCl_3$, 298 K).

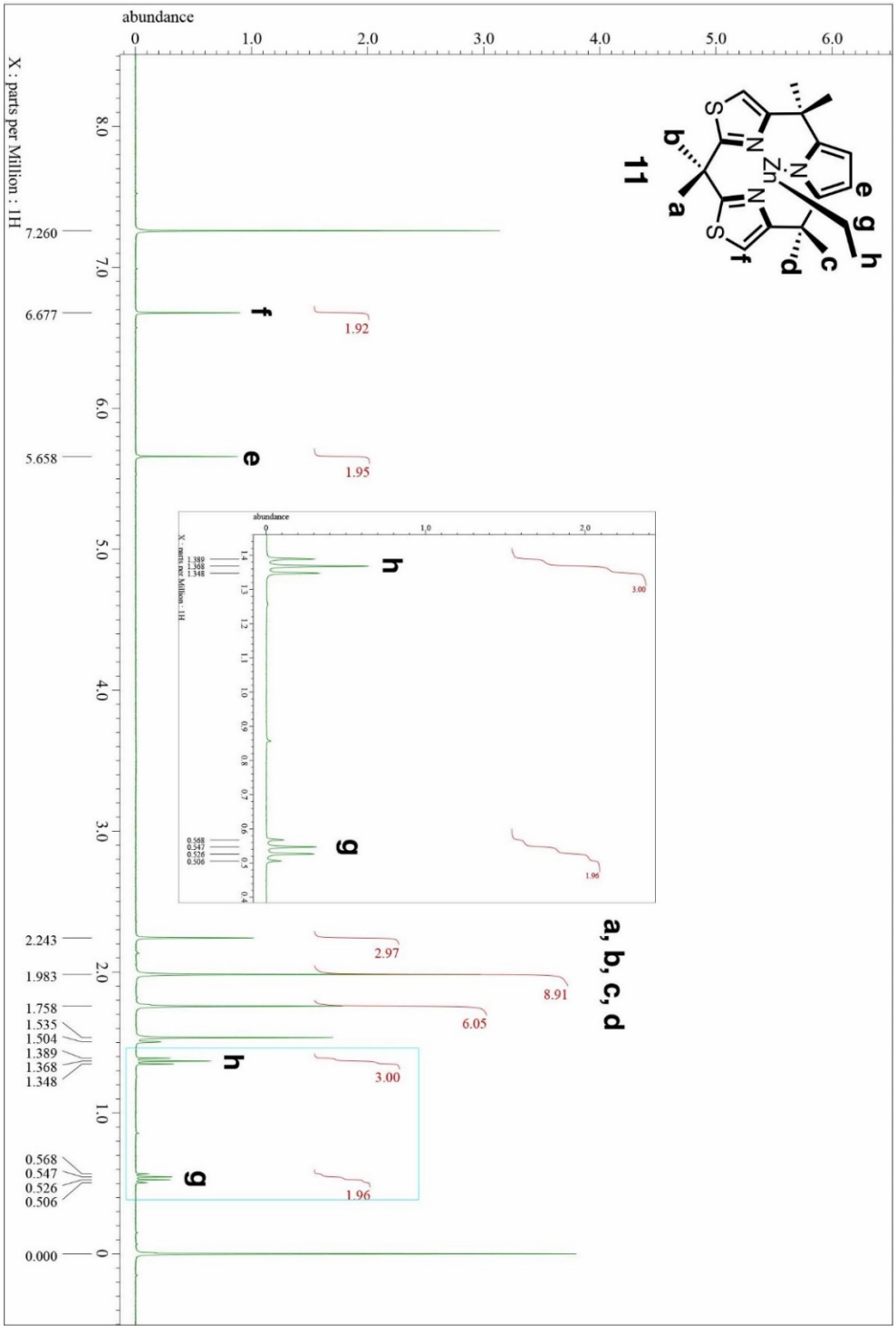

Figure S45. ^{1}H NMR spectrum of compound **11** (400 MHz, $CDCl_3$, 298 K).

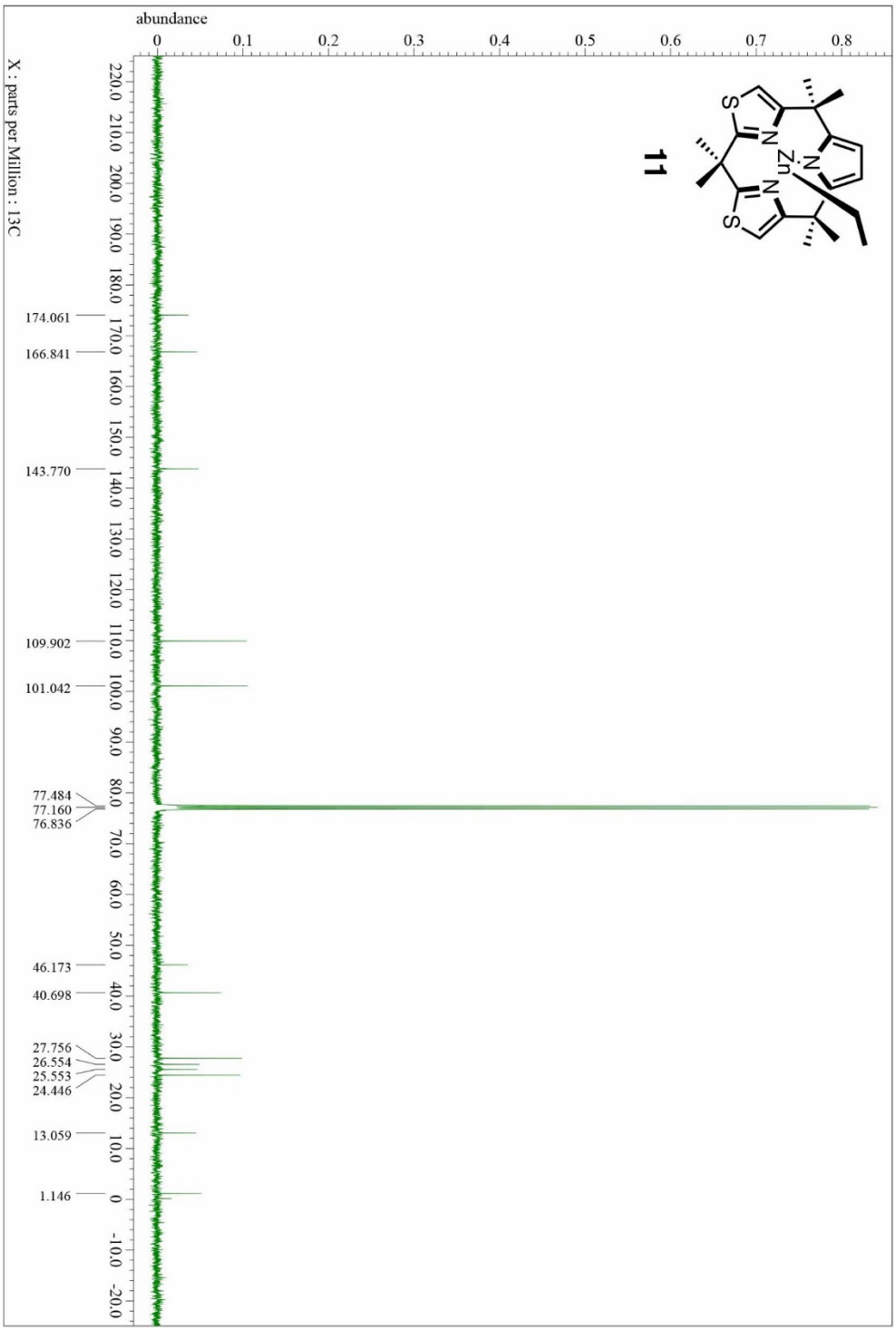

Figure S46. ^{13}C NMR spectrum of compound **11** (100 MHz, $CDCl_3$, 298 K).

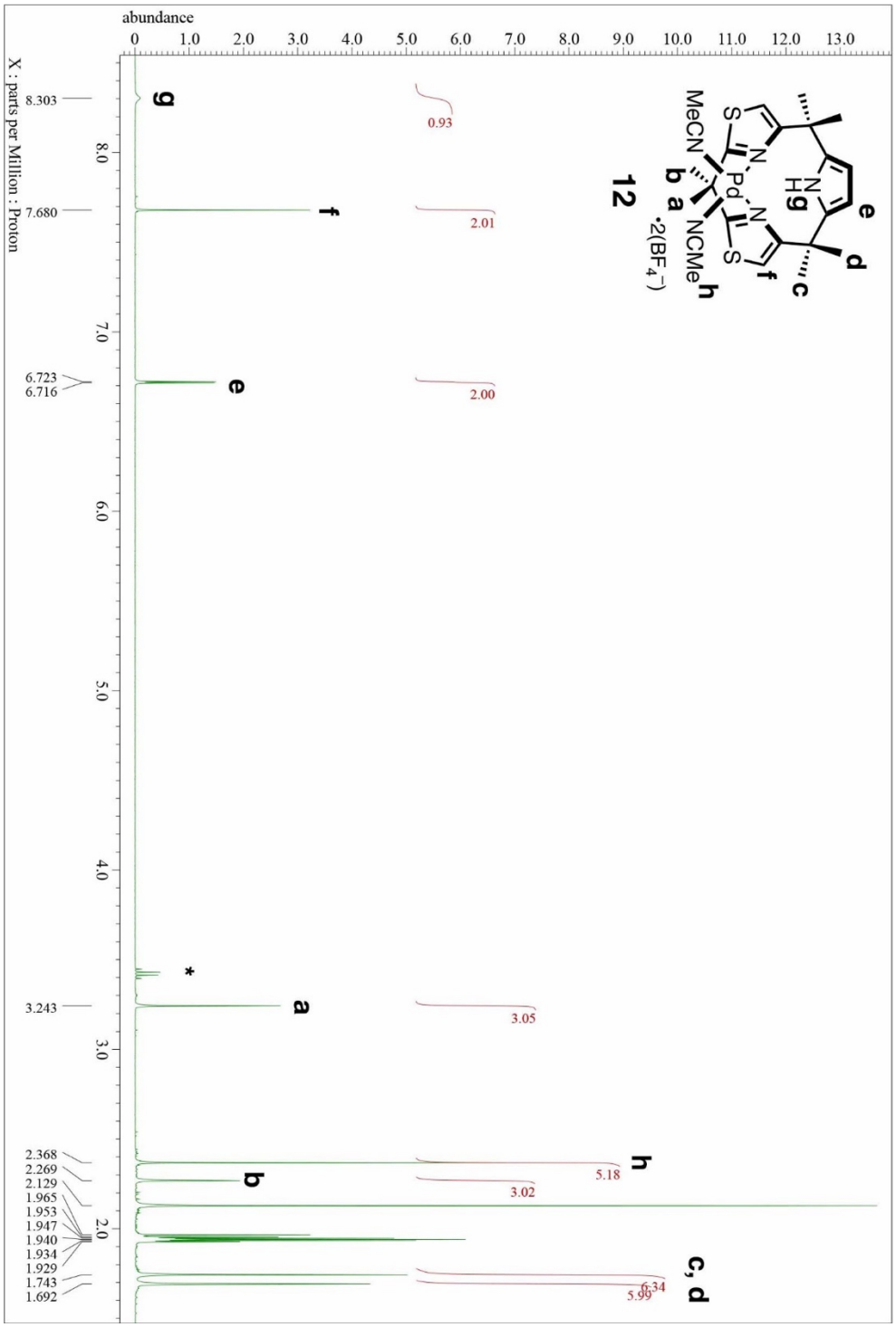

Figure S47. ^{1}H NMR spectrum of compound **12** (400 MHz, CD_3CN, 298 K).

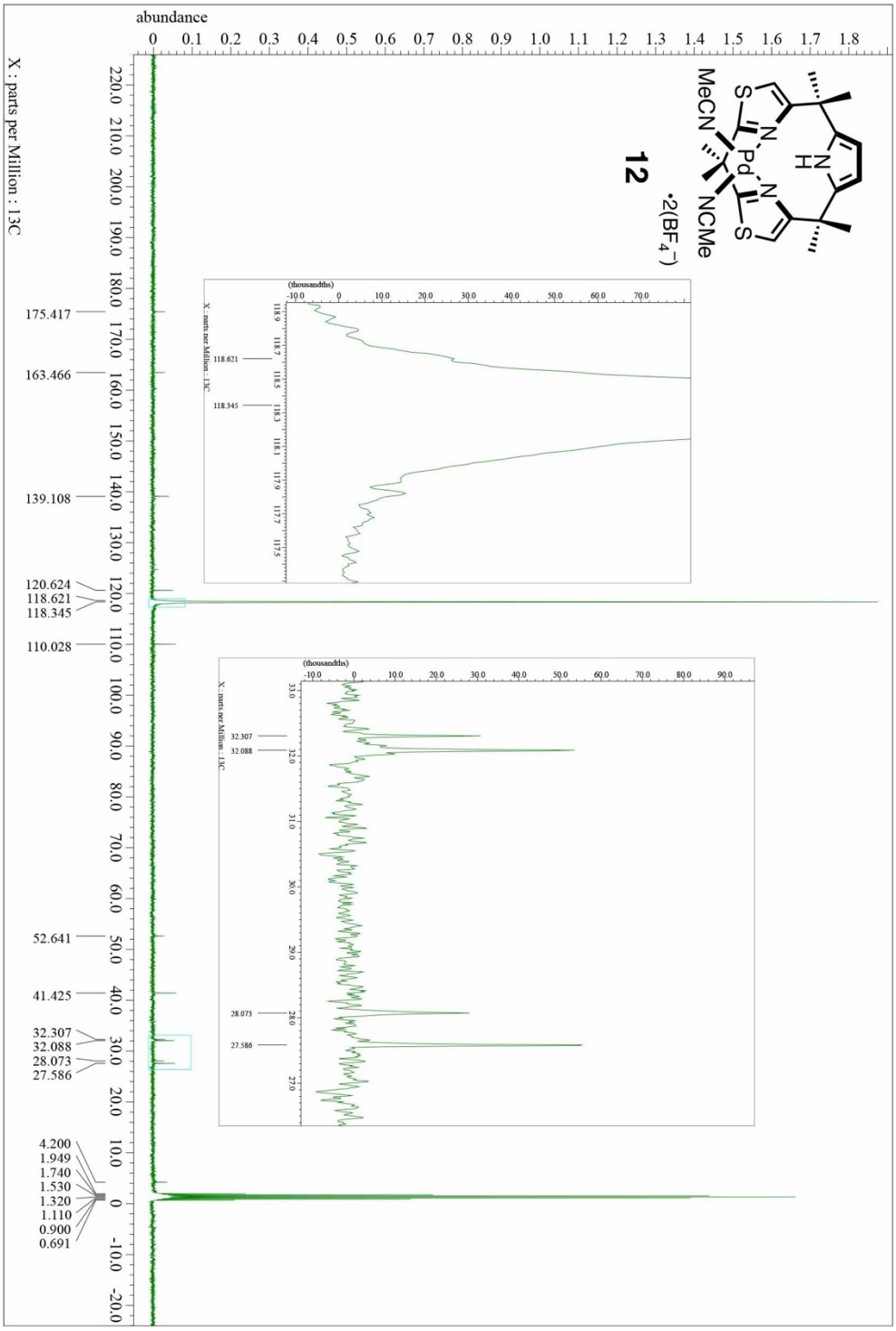

Figure S48. ^{13}C NMR spectrum of compound **12** (100 MHz, CD_3CN, 298 K).

9. Cartesian Coordinates for Optimized Structures

(A) With the M06-2X/6-311+G(2d,p) level of theory

Coordinate and total energy of the lowest energy conformer of each compound shown in **Figure S2-S7**.

Compound **1**

C	9.847006748070	2.643942489382	7.313460643600
C	10.320494546012	1.415760349014	6.526946038041
C	9.732257475642	3.840276754255	6.360707833456
C	8.518528355697	2.340700052558	7.980519891357
C	7.644544881056	1.284149261662	7.901800516948
C	6.717526873109	1.409342059385	8.978828929326
C	7.054679695661	2.531536956607	9.697230706239
C	6.733105730937	2.929654973056	11.130170479451
C	6.648606927283	4.454064708805	11.285376696590
C	5.408164745733	2.305994725493	11.561452437200
C	7.873974664840	2.348284105734	11.951988080151
C	8.006991482325	1.130198908928	12.574769363723
C	9.399269604016	0.889346836756	12.772182536786
C	10.082818299693	1.972687720553	12.276118525373
C	11.546043843388	2.231968779071	11.968625225525
C	12.145806263880	3.254352945080	12.941962182572
C	12.333068285870	0.919529057640	12.066897864061
C	11.582803103421	2.787949950317	10.556795702316
C	12.035140310234	3.982608649552	10.053327423339
C	11.545953767180	4.101985332374	8.714831408647
C	10.808971980732	2.976680372202	8.439622335717
N	8.110997861611	3.109600294000	9.039719755053
N	9.139466210849	2.864005715034	11.835547579890
N	10.878565882579	2.171690590369	9.550720969072
H	10.444706389488	0.551370962832	7.180440322413
H	11.277936732768	1.630663150337	6.050943385931
H	9.596065561180	1.159372853715	5.751268535151
H	9.038611295906	3.598997969492	5.554711794448
H	10.705121279019	4.077459734022	5.924942944382
H	9.360849594321	4.725596416614	6.879035019111
H	7.680023614337	0.487704702711	7.176104374091
H	5.936979119050	0.710674964100	9.231535364802
H	8.635271360193	3.911144329119	9.353034681268
H	7.571768264422	4.963690458466	10.997342021575
H	6.446187306757	4.711570046947	12.326000822147
H	5.847573771693	4.849419377737	10.658994769603
H	4.595997029752	2.688700672348	10.941879490626
H	5.202910725713	2.549342262114	12.604858618787
H	5.431367382483	1.221003596689	11.462269482283
H	7.203999266941	0.449166893157	12.804423272723
H	9.842010413939	0.004703806394	13.200654022905

H	9.389935910889	3.711424575864	11.351194374286
H	11.585383094156	4.190291674967	12.927147292993
H	13.184482957070	3.468259186064	12.681026844936
H	12.116229961097	2.853346082046	13.955523298148
H	12.259648902908	0.507967993583	13.075548194061
H	13.384448593120	1.103491413277	11.842637426970
H	11.953181500230	0.176733162773	11.364374548393
H	12.634137968689	4.704743392362	10.584220740944
H	11.706956772091	4.930623681197	8.044351644909
H	10.252271691991	1.391946053279	9.709201587654

Total energy = -980.613258829492 hartree

Compound **2**

C	3.761824702223	4.297811004847	4.224529941080
C	2.891869375557	4.297756806447	2.971269071663
H	2.253008952406	5.181859334056	2.959742379813
H	3.490309448413	4.297508548374	2.057275390256
C	2.893583285149	4.298025813147	5.487960005643
H	3.523273508841	4.298095990829	6.374859982695
H	2.260401171800	5.186504010993	5.499688623371
C	4.708348387826	5.495871274237	4.261600370859
S	5.103099412389	6.472292061547	2.881232429949
C	6.389408345624	7.187322907308	3.778418619522
H	7.039278230777	7.917042525711	3.325362388459
C	6.447801127383	6.651453416847	5.026698944417
N	5.449880684520	5.742513552500	5.288458612490
C	7.564635842167	6.780220492729	6.058047091657
C	6.962656359213	7.132976251008	7.426886870065
H	6.231390406129	6.386154842276	7.735084757277
H	6.463462648787	8.103491202880	7.381948090141
H	7.754254998601	7.175445105377	8.176379839035
C	8.567329332080	7.851863891940	5.641932843529
H	9.363191004868	7.921986138195	6.384531924563
H	8.076147511522	8.824400585744	5.572732872130
H	9.023157723957	7.617354981576	4.678651467770
C	8.250087388530	5.424061667560	6.100600510561
C	9.520359606568	5.011541329377	5.768685541830
H	10.355134526582	5.650979444449	5.530917413510
N	7.517181028622	4.297831362087	6.351109580798
H	6.505603949365	4.297763725630	6.398585902390
H	2.252712250385	3.413857230946	2.960021386405
H	2.260302734412	3.409623710276	5.499911163623
C	4.708148871470	3.099588320675	4.261821031478
S	5.102127066826	2.122337386231	2.881808007026
C	6.388624402214	1.407492494600	3.778858989155
H	7.038128388715	0.677307376858	3.325972701070
C	6.447684245421	1.944053508490	5.026823720851
N	5.450045279175	2.853321491745	5.288508739334
C	7.564858077806	1.815430512972	6.057825953421
C	6.963376528643	1.462357988619	7.426815391840
H	6.232116477793	2.209052401186	7.735329653373
H	6.464308452406	0.491773975285	7.381890626068
H	7.755229679337	1.419920459547	8.176030291086
C	8.567639926180	0.744047245024	5.641241503854
H	9.363764869579	0.674023717610	6.383560856366
H	8.076665093619	-0.228585815530	5.572117968702
H	9.023095811158	0.978779063871	4.677862141721
C	8.250137292364	3.171673710421	6.100404826840
C	9.520388654381	3.584310390761	5.768566306341
H	10.355215938230	2.944931562734	5.530778275990

Total energy = -1698.393476977605 hartree

Compound **3**

C	3.949966368802	4.336834396715	3.786593650897
C	3.906602916486	4.609383471006	2.281216662018
C	2.540069368503	4.098316478947	4.334459190488
C	4.639401609831	5.484489096989	4.504318614573
C	5.171644060044	6.812299419621	6.183582075440
C	6.271490392473	6.559197371249	5.410141362794
C	7.734396594100	6.765251486440	5.742332206349
C	7.875668510975	7.607298409977	7.016563005628
C	8.451684299781	7.458014422515	4.578814842367
C	8.324909589319	5.375413441740	5.947196241220
C	9.582683837739	4.854421354833	5.746857093451
C	4.848942217785	3.152036550834	4.103531644729
C	6.421410160435	1.625964738359	3.837726211495
C	6.359935749327	2.015992940172	5.145959681538
C	7.391950142914	1.845851786868	6.248634173317
C	6.696822242281	1.635964407065	7.600257124930
C	8.315879099747	0.669141607297	5.948733586066
C	8.189377370404	3.142420772666	6.235903470593
C	9.496622810527	3.440064175011	5.927090107009
N	5.908651305018	5.759844446933	4.350127047635
N	7.518941022667	4.330948790210	6.302015707591
N	5.342032912788	2.930999791783	5.295965706450
N	5.450370416271	2.356504103059	3.185283501576
N	4.133326622891	6.127313228820	5.589402081405
H	3.267353395356	5.469628772693	2.080480596786
H	4.905220418654	4.832365964933	1.904436618649
H	2.575989296830	3.826691219530	5.390518821273
H	1.917216854618	4.987173823762	4.203425053287
H	5.037573136643	7.382110266812	7.086348338667
H	7.414979406775	7.106320605893	7.869892137800
H	7.410879443811	8.588379849454	6.886997339349
H	8.932233614087	7.751539407069	7.244524580196
H	9.520427944974	7.537231170479	4.785216890493
H	8.051525129792	8.464442941392	4.439450188215
H	8.313113594446	6.890073022286	3.659533009803
H	10.464878195248	5.409961060950	5.471603309938
H	6.509286173784	4.367775067723	6.298911538881
H	3.490330934441	3.753336671690	1.743178052589
H	2.068349508422	3.276279415512	3.795216142603
H	7.071348414618	0.947599392931	3.314005110969
H	6.019275719763	2.460569843274	7.821030485419
H	6.114346658168	0.711961594688	7.586377003506
H	7.442622965588	1.574630299829	8.394264890539
H	9.075024260456	0.582627000340	6.727860942299
H	7.745242293962	-0.260773992137	5.917089489971
H	8.828107066973	0.801201811919	4.994257044561
H	10.298062667025	2.729430210601	5.802349170057
H	5.284754460791	2.365182741575	2.192790462139
H	3.197378822675	6.041495146690	5.948937791448

Total energy = -1012.720760669164 hartree

Compound **4**

C	3.762703518603	4.298017476044	4.252037840177
C	3.075487824158	4.297951990292	2.890041834540
C	2.755328897006	4.298369448535	5.403809912981
C	4.715455016549	5.470723503396	4.411063076543
C	6.309369361998	6.771231516777	3.782385848845
C	6.405467981332	6.570934589713	5.114780423714
C	7.559700811251	6.780935402592	6.074658106470
C	7.033542429264	7.221451970777	7.447036823133
C	8.530924478176	7.821791074260	5.523879155783
C	8.248614159276	5.425209478488	6.156066886367
C	9.519147524303	5.011329836814	5.829954742357
C	4.715017388701	3.124985330678	4.411322052503
C	6.307889039224	1.823105221852	3.782820490350
C	6.404936863876	2.024591488253	5.114970962405
C	7.559426677440	1.814674609185	6.074530602755
C	7.033545581310	1.374141600724	7.447023851359
C	8.530507052984	0.773855243159	5.523439726473
C	8.248417080579	3.170367233616	6.155863415249
C	9.519018748973	3.584086159899	5.829836966954
O	5.229979320086	6.066337589784	3.318939633832
O	5.228536266587	2.528101053707	3.319408482231
N	5.333316373848	5.773630387625	5.498561133346
N	5.333412191122	2.822724093428	5.498685173614
H	2.446306472356	5.183538542388	2.796957698476
H	3.797851335790	4.297873802249	2.075816867789
H	3.274179381061	4.298303906024	6.360166941908
H	2.125602315434	5.186388192052	5.340066937046
H	6.882448160624	7.313383226412	3.052601837171
H	6.331032164547	6.490946710057	7.847318052676
H	6.519594872499	8.181766180381	7.366165417153
H	7.866893776736	7.322455149117	8.143475831091
H	9.379746958075	7.934290338981	6.199897634679
H	8.033592692434	8.788795748867	5.431778416013
H	8.915826920930	7.526874647985	4.546133719669
H	10.352240142926	5.650487263351	5.585679785655
N	7.512447872390	4.297835645256	6.399962148379
H	6.504750954415	4.297909051904	6.503048240648
H	2.446253127709	3.412360551781	2.797062843568
H	2.125075911774	3.410712057369	5.340188180336
H	6.880165937299	1.279758094912	3.053254220987
H	6.330671160764	2.104361307608	7.847176600355
H	6.520102797088	0.413536805169	7.366355415715
H	7.866972765024	1.273740532051	8.143475930308
H	9.379497357065	0.661185324700	6.199222170858
H	8.033119838402	-0.193109652243	5.431299506773
H	8.915177369568	1.068908080686	4.545649718503
H	10.352005128416	2.944852193299	5.585428742248

Total energy = -1052.438266316848 hartree

Compound **5**

C	2.263196383971	7.972829388013	4.900803120419
C	1.579025791698	9.061458329057	4.467643736066
C	0.937097659463	9.623353421285	5.622745599863
C	1.284669581412	8.837425262417	6.671070680143
C	0.873809319399	8.772987864498	8.124205704366
C	1.938474269090	9.431232579382	9.009722332282
C	-0.469636915320	9.489720564059	8.298677765917
C	0.728386067240	7.297535356359	8.456214139983
C	1.405760107712	6.600995994583	9.406682492948
C	0.136447097745	5.261893993390	7.832352101290
C	-0.318058500436	4.206138288653	6.836740634761
C	0.100930577230	2.794805205437	7.260487133867
C	-1.840110571815	4.282149368356	6.669694828842
C	0.386104366311	4.593849795536	5.539151790955
C	1.040396687851	5.220441013644	3.280990839155
C	1.834978072405	5.696090266631	4.275997571733
C	2.893461178960	6.791413222564	4.197289384738
C	3.201110381769	7.157158659761	2.748816477880
C	4.166459586314	6.343170118181	4.924917883030
N	-0.024911454023	6.522581541290	7.609912447346
N	1.476128001036	5.277355285814	5.531250516844
O	2.123074280041	7.861655595109	6.245408969440
S	1.155001659263	4.913834170537	9.193524234948
S	-0.250376224077	4.289953069976	3.947397808261
H	1.493702009592	9.400157918779	3.448620582572
H	0.274337173067	10.471994535758	5.649507609618
H	2.911131764817	8.957720830509	8.868505592553
H	1.659940948148	9.360218065553	10.063766539517
H	2.029306090101	10.486128761219	8.749313421308
H	-0.386550781352	10.535193518164	7.995029468213
H	-0.768570694071	9.460425084119	9.347599849617
H	-1.238979283361	9.005894854991	7.697401493306
H	2.061904632956	6.971030474555	10.176237838984
H	-0.236095504240	2.072054544192	6.516363373366
H	-0.350944132457	2.534212647005	8.220243158313
H	1.185663212922	2.717282106651	7.344671842894
H	-2.141189036418	5.289002023138	6.383148104298
H	-2.325207919853	4.022597977239	7.611724664673
H	-2.176972042835	3.576733777497	5.906626972051
H	1.095945994208	5.404588934975	2.220995368418
H	3.939929693035	7.958575719191	2.714559791315
H	2.307340449871	7.494236593786	2.221152630024
H	3.605827459130	6.290804238112	2.222557540119
H	4.901589038951	7.149936897755	4.922915974254
H	4.594651728119	5.474525234373	4.421159060794
H	3.937909346430	6.073662366902	5.954899170718

Total energy = -1718.243401246692 hartree

Compound **10**

C	0.303019507946	4.646883719332	4.420699541246
C	-0.521996805938	3.548557349503	3.756350124492
H	-0.668461713119	2.716277103425	4.445731830327
H	0.001022725649	3.173920016334	2.874813888521
H	-1.498507167878	3.919996427820	3.441849105216
C	1.680795958204	4.107900897873	4.832940104727
H	2.284244314360	4.897008678617	5.280146087665
H	2.202766426071	3.728320692662	3.953438064468
H	1.569582902591	3.297993868286	5.556403678615
C	-0.434393375531	5.180808051837	5.634197547070
C	-1.741126994384	5.232107598695	5.990381188072
H	-2.554982120924	4.721383347121	5.503567945125
C	-1.834717690688	6.146917428561	7.095980950779
H	-2.731772099488	6.460599301943	7.603413627266
C	-0.577098730980	6.584792929263	7.342781684403
O	0.286156533797	5.955232780706	6.495230337531
C	0.007259838891	7.724654687875	8.153432285761
C	1.348156273101	7.298726109703	8.775229257472
H	1.195167101808	6.446367703591	9.439242344872
H	1.766697662765	8.126650755289	9.348733074559
H	2.064253315338	7.011684421809	8.005530582005
C	-0.973297394060	8.143052214538	9.245454498857
H	-1.924211718746	8.467171478377	8.820916601044
H	-0.556582150945	8.967430639550	9.826330406196
H	-1.155269442607	7.307839442091	9.922403402989
C	0.246285217408	8.888320623867	7.190369557508
C	0.001036218127	10.206129825191	7.293569012104
H	-0.389439046844	10.749209898614	8.136762199609
S	0.359093752188	11.045140467725	5.787593224053
C	0.769571312613	9.523229860194	5.010887882852
N	0.766384305143	8.565551158369	5.958443953311
H	0.911882684356	7.607564642150	5.586150126373
N	0.919196129103	9.347349911276	3.720723831614
C	0.840599613902	8.048089335271	3.303508851175
S	0.368072048390	7.631922194637	1.668965375591
C	0.167306902790	5.974864012968	2.164125381621
H	-0.197327234880	5.234121497093	1.472111479824
C	0.482950389648	5.836358559716	3.475034146949
N	0.927692552813	6.986423368126	4.063018818127

Total energy = -1655.675273242112 hartree

Coordinate and total energy of Pd(II) complex shown in **Figure S17**.

Pd(II) complex **12**

H	4.640730000	8.281960000	5.261210000
H	3.759820000	9.417460000	7.549720000
H	2.318430000	8.722180000	9.528870000
H	0.826610000	9.525610000	10.060350000
H	1.998090000	10.403790000	9.057890000
H	0.191360000	10.928230000	7.324730000
H	-0.948400000	10.181590000	8.455400000
H	-0.906380000	9.640290000	6.766510000
H	-1.838630000	8.177790000	9.021110000
H	0.451110000	7.883000000	5.445930000
H	1.405360000	2.243730000	7.478080000
H	0.873700000	2.940730000	9.020520000
H	2.215430000	3.668520000	8.134290000
H	-1.899790000	3.701960000	6.663300000
H	-1.445750000	2.951490000	8.212630000
H	-0.899070000	2.230230000	6.703840000
H	0.644740000	4.981550000	2.447690000
H	0.618040000	7.778440000	2.875750000
H	1.626820000	6.848800000	1.738000000
H	2.165610000	8.436620000	2.299960000
H	4.355800000	7.332530000	2.929510000
H	3.708630000	5.741360000	2.481010000
H	4.386250000	6.000090000	4.103830000
H	5.306960000	7.734750000	11.051680000
H	5.156840000	6.006240000	11.507970000
H	3.871940000	7.179010000	11.968450000
H	6.939150000	4.294600000	5.216120000
H	6.172870000	2.820860000	5.894760000
H	7.074540000	3.912630000	6.972280000
C	2.517900000	7.868710000	4.919640000
C	3.610060000	8.372760000	5.576410000
C	3.145920000	8.969260000	6.780010000
C	1.781360000	8.806250000	6.831240000
C	0.802840000	8.958180000	7.970470000
C	1.536880000	9.426360000	9.233950000
C	-0.289520000	9.986110000	7.602440000
C	0.129120000	7.609760000	8.231920000
C	-1.130730000	7.422980000	8.710070000
C	-0.115780000	5.368290000	7.934950000
C	0.182930000	4.018120000	7.269150000
C	1.245840000	3.180760000	8.019940000
C	-1.099090000	3.184400000	7.201040000
C	0.647870000	4.376950000	5.861410000
C	0.818130000	4.904910000	3.511110000
C	1.627400000	5.670540000	4.275640000
C	2.407960000	6.890350000	3.783750000
C	1.647020000	7.522130000	2.601730000
C	3.806720000	6.460660000	3.299520000

C	3.935850000	6.605010000	9.960780000
C	4.609690000	6.909750000	11.210130000
C	5.230340000	4.606600000	6.379400000
C	6.435220000	3.863860000	6.083600000
N	0.702860000	6.397240000	7.864870000
N	1.400870000	8.200710000	5.658450000
N	1.553290000	5.304570000	5.614680000
N	3.406130000	6.392430000	8.986040000
N	4.281260000	5.183260000	6.600220000
S	-1.619900000	5.794770000	8.600350000
S	-0.079130000	3.803500000	4.443850000
Pd	2.542330000	5.936350000	7.228320000
B	6.023590000	3.535800000	9.763720000
B	-2.180670000	7.482760000	4.907080000
F	5.411810000	3.907460000	10.949860000
F	6.654240000	4.634740000	9.209020000
F	6.954170000	2.558460000	10.041060000
F	5.061100000	3.085110000	8.896540000
F	-1.209410000	6.735800000	5.493970000
F	-2.809780000	8.220540000	5.851200000
F	-3.151920000	6.735800000	4.320190000
F	-1.551560000	8.220540000	3.962960000

Total energy = -2939.981208542782 hartree

(B) With the B3LYP+D3/6-311+G(2d,p) level of theory

Coordinate and total energy of compounds **1**, **2**, and **4** shown in **Figure S17**.

Compound **1**

C	9.853405811388	2.633084699737	7.307113953189
C	10.338658926208	1.393982475646	6.531161003932
C	9.729299529155	3.821319490966	6.334161374834
C	8.519316514217	2.335069224315	7.976301654945
C	7.634466058470	1.281833842580	7.900583726096
C	6.705045445666	1.415542066421	8.974713720977
C	7.043621279560	2.541437038567	9.695529334599
C	6.727113646884	2.939345128069	11.135324094116
C	6.649951959420	4.471375211778	11.294315214370
C	5.388797081988	2.330689864179	11.571787478047
C	7.869298750406	2.348365108765	11.958499202984
C	8.007881450040	1.112871245175	12.555340477801
C	9.400177091662	0.868859352709	12.749166415798
C	10.088947049961	1.964837525994	12.277477234389
C	11.556274295332	2.229228104727	11.971748644757
C	12.151486940400	3.246799466795	12.963841537470
C	12.354452707220	0.914477779351	12.057699626366
C	11.595311305773	2.796141110972	10.559788221226
C	12.004590331508	4.014580039457	10.066166233673
C	11.515504113646	4.130746171968	8.726691767088
C	10.818254592759	2.980707090833	8.431814538812
N	8.108623277981	3.111556816371	9.034912496226
N	9.140345345211	2.867386858478	11.856089453815
N	10.919014211901	2.163429165471	9.537971870407
H	10.462458259531	0.534769105048	7.191997447513
H	11.299804585465	1.605519900277	6.059806420550
H	9.623752593909	1.122813261311	5.751161128552
H	9.031966773832	3.568785539416	5.534141223312
H	10.697180891639	4.062108768855	5.888065456414
H	9.354734048240	4.711986266562	6.841358903951
H	7.662018087022	0.483388844323	7.176758500931
H	5.922106835531	0.718640620711	9.224987054575
H	8.639115881296	3.904578214526	9.352731224087
H	7.572455106452	4.980275612431	11.001876376694
H	6.454188855896	4.731817671264	12.336091813511
H	5.848041446084	4.874107874062	10.672833301720
H	4.578767954259	2.721223610680	10.953540675835
H	5.185456956751	2.578589480407	12.614911555274
H	5.391482941805	1.244923635371	11.477639305055
H	7.208433150041	0.422211492192	12.767892254148
H	9.839701889157	-0.025144039970	13.161205827191
H	9.388208544702	3.723506197487	11.390307112675
H	11.590354390055	4.182688049085	12.956492197206
H	13.192352406743	3.468724128114	12.716563423715
H	12.114771200500	2.837933992142	13.974564204622
H	12.290698170808	0.489450887940	13.061837539467

H	13.404585936492	1.103467815272	11.829119105873
H	11.977376154615	0.173854986819	11.350913104967
H	12.577368885753	4.753556066343	10.602548349574
H	11.652274014477	4.973168629040	8.068316438671
H	10.319350322196	1.365109509976	9.687408776996

Total energy = -981.073017484224 hartree

Compound **2**

C	3.752311352119	4.297716474796	4.222234849075
C	2.853528140331	4.297702280999	2.981575812166
C	2.891540973491	4.297707813380	5.499677935105
C	4.701611107891	5.501125011806	4.247487857918
C	6.401636036273	7.193938926449	3.759300077901
C	6.453645275168	6.661923515272	5.013729368432
C	7.569914947054	6.789743903866	6.054870775076
C	6.958427004352	7.146792097746	7.427133524845
C	8.578440724732	7.869136558411	5.648403479650
C	8.255106347783	5.429085092822	6.104097500306
C	9.531670723209	5.011915406764	5.786503125822
C	4.701653796784	3.094341634020	4.247486141099
C	6.401778048732	1.401645117583	3.759265583745
C	6.453739178838	1.933613800602	5.013713931675
C	7.570030530108	1.805836126191	6.054839356811
C	6.958592674175	1.448737806135	7.427109985235
C	8.578608880811	0.726505119949	5.648332655069
C	8.255156177689	3.166528341296	6.104074967378
C	9.531702583258	3.583761405673	5.786488914395
N	5.450069767379	5.756234116521	5.271872815281
N	7.517750726028	4.297787341416	6.348443428953
N	5.450107037176	2.839235703108	5.271877985413
S	5.109338194581	6.479095387368	2.850084677482
S	5.109454390152	2.116452111748	2.850060664831
H	2.213741074033	5.181358438766	2.981801837491
H	3.427905028429	4.297704328620	2.052375608213
H	3.522877995378	4.297718355746	6.384945097823
H	2.256701560453	5.185653611813	5.517965064938
H	7.053988651467	7.920672191735	3.304904329635
H	6.225307757887	6.401945278321	7.735159158955
H	6.459099780760	8.118197417574	7.381891712428
H	7.745187477155	7.190358347857	8.182619144438
H	9.368419902722	7.942740377006	6.397164755152
H	8.087529588401	8.841773390609	5.574944415250
H	9.046590487570	7.641519982488	4.689330271530
H	10.373032917662	5.647788123785	5.562709477116
H	6.504087017473	4.297764920927	6.346747617942
H	2.213758492134	3.414033907146	2.981810101228
H	2.256722673914	3.409747405799	5.517970444251
H	7.054173082021	0.674958882571	3.304854567620
H	6.225437566985	2.193539722672	7.735159414559
H	6.459321273982	0.477303841749	7.381869811030
H	7.745373294963	1.405210364655	8.182577125477
H	9.368613317462	0.652938687136	6.397069241967
H	8.087753558898	-0.246158913528	5.574872673271
H	9.046717502434	0.954163418242	4.689250328696
H	10.373094379695	2.947931825395	5.562683387322

Total energy = -1698.872342415890 hartree

Compound **4**

C	3.753750027176	4.297945254751	4.249486936708
C	3.056861707166	4.297956413195	2.885414518018
C	2.736530215135	4.298065938027	5.402195201790
C	4.705841304798	5.477244507098	4.406275998286
C	6.312815772415	6.785185416098	3.773456156663
C	6.408340120121	6.583225000752	5.109492117265
C	7.565760917000	6.790436392421	6.075597167795
C	7.037690024812	7.231017423290	7.455591005093
C	8.540229310927	7.841821121080	5.531766858272
C	8.255567209841	5.430217545430	6.158083313833
C	9.526667949130	5.011446890080	5.823719013753
C	4.705662935999	3.118511429141	4.406348622043
C	6.312497942545	1.810363660977	3.773592503938
C	6.408001691164	2.012327114846	5.109633145941
C	7.565391854287	1.805000021712	6.075752623708
C	7.037267995701	1.364581247563	7.455776671979
C	8.539705057521	0.753441532994	5.531978648647
C	8.255400763323	3.165121705657	6.158153999411
C	9.526563116425	3.583684127573	5.823763333619
O	5.225855058880	6.076204217967	3.304050517313
O	5.225644528660	2.519475425230	3.304142701690
N	5.333816788328	5.784761088807	5.491933637424
N	5.333564245139	2.810931300671	5.492033371122
H	2.426473104574	5.183346600120	2.792644296671
H	3.774185085876	4.297872755878	2.066677709427
H	3.244927380048	4.298055467271	6.364029335757
H	2.104965454263	5.185552791578	5.336483100318
H	6.884748223814	7.325671886809	3.041853201715
H	6.333083510280	6.502935167943	7.856321475979
H	6.525866956316	8.193992118518	7.381003171266
H	7.870314939896	7.328307252126	8.154491164575
H	9.386580144864	7.957798712833	6.210541123989
H	8.041025914726	8.808387684569	5.440136297766
H	8.933159429220	7.557285113187	4.553989533970
H	10.362187645131	5.647180102755	5.578868099111
N	7.520141837277	4.297731087079	6.411215166819
H	6.509658790038	4.297809846539	6.484853820370
H	2.426332167298	3.412660496315	2.792702918803
H	2.104815838870	3.410681365386	5.336543180497
H	6.884379363157	1.269783918262	3.042015071523
H	6.332767714678	2.092788740971	7.856466193088
H	6.525308739883	0.401673232906	7.381255688494
H	7.869885680637	1.267219689925	8.154676134305
H	9.386043959995	0.637381730105	6.210754270346
H	8.040360463922	-0.213057493153	5.440406778443
H	8.932671857994	1.037863949383	4.554183005477
H	10.361989258752	2.947813007336	5.578951196979

Total energy = -1052.901735390664 hartree

10. References

1. H. Fujita, S. Arai, H. Arakawa, K. Hamamoto, T. Kato, T. Arai, K. Hotta, N. Hosokawa, T. Ohbayashi, C. Takahashi, Y. Inokuma, I. Tamai, S. Yano, M. Kunishima and Y. Watanabe, *ChemRxiv*, 2023, doi: 10.26434/chemrxiv-2023-ps4h1.
2. G. M. Sheldrick, *Acta Crystallogr. Sect. A*, 2015, **71**, 3–8.
3. G. M. Sheldrick, *Acta Crystallogr. Sect. C*, 2015, **71**, 3–8.
4. S. Maeda and Y. Harabuchi, *WIREs Comput. Mol. Sci.*, 2021, **11**, e1538.
5. AFIR web, https://afir.sci.hokudai.ac.jp
6. J. J. P. Stewart, *J. Mol. Model.*, 2007, **13**, 1173–1213.
7. Y. Zhao and D. G. Truhlar, *Chem. Account*, 2008, **120**, 215–241.
8. Gaussian 16, Revision C.01, M. J. Frisch, G. W. Trucks, H. B. Schlegel, G. E. Scuseria, M. A. Robb, J. R. Cheeseman, G. Scalmani, V. Barone, G. A. Petersson, H. Nakatsuji, X. Li, M. Caricato, A. V. Marenich, J. Bloino, B. G. Janesko, R. Gomperts, B. Mennucci, H. P. Hratchian, J. V. Ortiz, A. F. Izmaylov, J. L. Sonnenberg, D. Williams-Young, F. Ding, F. Lipparini, F. Egidi, J. Goings, B. Peng, A. Petrone, T. Henderson, D. Ranasinghe, V. G. Zakrzewski, J. Gao, N. Rega, G. Zheng, W. Liang, M. Hada, M. Ehara, K. Toyota, R. Fukuda, J. Hasegawa, M. Ishida, T. Nakajima, Y. Honda, O. Kitao, H. Nakai, T. Vreven, K. Throssell, J. A. Montgomery, Jr., J. E. Peralta, F. Ogliaro, M. J. Bearpark, J. J. Heyd, E. N. Brothers, K. N. Kudin, V. N. Staroverov, T. A. Keith, R. Kobayashi, J. Normand, K. Raghavachari, A. P. Rendell, J. C. Burant, S. S. Iyengar, J. Tomasi, M. Cossi, J. M. Millam, M. Klene, C. Adamo, R. Cammi, J. W. Ochterski, R. L. Martin, K. Morokuma, O. Farkas, J. B. Foresman, and D. J. Fox, Gaussian 16, Revision C.01; Gaussian, Inc., Wallingford CT, 2016.
9. C. E. Colwell, T. W. Price, T. Stauch and R. Jasti, *Chem. Sci*., 2020, **11**, 3923–3930.
10. Visual Molecular Dynamics. https://www.ks.uiuc.edu/Research/vmd/.
11. D. Andrae, U. Haeussermann, M. Dolg, H. Stoll and H. Preuss, *Theor. Chem. Acc.*, 1990, **77**, 123–141.
12. J. Contreras-García, E. R. Johnson, S. Keinan, R. Chaudret, J.-P. Piquemal, D. N. Beratan and W. Yang, *J. Chem. Theory Comput*., 2011, **7** (3), 625–632.
13. G. J. Jones and A. Robertazzi, *J. Phys. Chem. B*, 2013, **117** (12), 3315−3322.
14. (a) A. D. Becke, *J. Chem. Phys.* 1998, **98**, 5648. (b) J. Stephens, F. J. Devlin, C. F. habalowski, and M. J. Frisch, *J. Phys. Chem.* 1994, **98**, 11623. (c) S. Grimme, J. Antony, S. Ehrlich, and Helge Krieg, *J. Chem. Phys.* 2010, **132**, 154104.
15. J.-D. Chai and M. Head-Gordon, *Phys. Chem. Chem. Phys.* 2008, **10**, 6615–6620.